Responses to the Anonymous Referee's comments

Referee #1 Evaluations:

The manuscript reports an optimized method to analyze the ^{13}C in the WSOC with small amounts, then applied it in the high time resolution aerosol samples during the haze period, and try to explain the source and processes beyond the variations of $\delta^{13}C$-WSOC. Although the context of this study does not introduce a bran-new method to analyze the carbon isotope or the new atmospheric process beyond what has been known, the optimized method will be a valuable contribution to the knowledge of WSOC. Overall, the manuscript is organized and read well. The paper does have a number of major issues that need to be addressed before publication.

Response: We thank the reviewer for the nice summary of our paper and the positive assessment of this work. We have carefully revised the manuscript following the reviewer comments and suggestions. Our responses to all comments made by the reviewer are given below (in blue font). And the revised parts are also shown after the responses (in green font). Please refer to the revised manuscript, in which changes are highlighted in yellow.

Major comments:

(1) The manuscript set up an optimized method, and declare it is novel, but limited information for previous method (e.g. the theory, operation, use condition and deficiency...) present in the introduction section. Thus, the reader cannot get the challenge or difficulty for the establish of new method. Try to add the previous researches in the introduction, the challenge of the new method in the abstract, and the comparison in the discussion section.

Response: We agree with the reviewer; the information of the previous methods was added in the introduction part. The importance of the optimized method was briefly stated in the abstract. Please see line 18-20 and line 99-117 in the revised MS.

In the abstract, we added "However, the previous methods measuring the $\delta^{13}C$

values of WSOC in ambient aerosols require large amount of carbon contents as well as time-consuming and labor-intensive preprocessing."

In the introduction, we added "This is partially due to the limited techniques to analyze the $\delta^{13}C$ signatures of WSOC in ambient aerosols, as their concentrations are usually very small. In the recent years, some efforts have been made to measure the $\delta^{13}C$ values of WSOC. Bauer et al. (1991) uses potassium persulfate to convert organic carbon in natural waters into CO_2 for $\delta^{13}C$ measurements. This wet oxidation method requires more than 0.5mM C and 1h during the pretreatment (from sample injection to the isolation of purified CO_2). Fisseha et al. (2006) boiled the oxidizing solution for 45 min to remove the organic matter and the total time required for the pretreatment (for 15 samples) is 1.5h. Kirillova et al (2010) develops a combustion method that applies the aerosol extract without filtration for isotope measurement and involves complicated processes such as the freeze-drying of the aerosol extract under vacuum for 16 h. This combustion method is the most widely used for the $\delta^{13}C$ measurements in WSOC aerosols (Kirillova et al., 2010, 2013, 2014; Miyazaki et al., 2012; Pavuluri et al, 2017). Although these methods are able to provide the $\delta^{13}C$ values of WSOC in natural waters and/or ambient aerosols, the analytical methods require either large amount of WSOC (from 100 μg C to 0.5 mM C) or time-consuming preprocessing. And some of the methods oxidize the WSOC extract without filtration and/or decarbonation in the pretreatment., which would result in higher uncertainty of the $\delta^{13}C$ results. The high detection limit of the previous methods is difficult to determine the $\delta^{13}C_{\text{-WSOC}}$ in aerosol samples with low carbon concentrations. In that case, an easily operated method detecting the $\delta^{13}C_{\text{-WSOC}}$ values in aerosol samples with low detection limit and high precision is urgently needed. "

(2) Line 55-65: The isotope signatures of particulate matter (not the WSOC, or VOCs) emitted from different sources have limited the various of isotope signatures of $\delta^{13}C$-WSOC, due to the most part of the WSOC come from the secondary formation rather than the primary emission. In addition, the isotopic effects during the formation or aging process is absence of proof, need add some reference.

Response: Thanks for the reviewer's suggestion, the possible sources and the corresponding isotope compositions were introduced more clearly in the introduction. And the atmospheric processes and their isotopic effect were described in more detail with corresponding references (Atkinson R., 1986; Kirillova et al., 2013; Fisseha et al., 2009; Nina et al., 1979; Rudolph et al., 2002; Sakugawa and Kaplan, 1995, Fisseha et al., 2009; Pavuluri and Kawamura, 2012; Iannone et al., 2003; Rudolph et al., 2000; Anderson et al., 2004; Fisseha et al., 2009; Rudolph et al., 2003) in a separate paragraph. Please see line 73-94 in the revised MS.

We added "In addition, atmospheric processes like secondary formation and photochemical aging may change the constitution and properties of WSOC, as well as the stable carbon isotope of WSOC ($\delta^{13}C_{\text{-WSOC}}$). According to the kinetic isotope effect (KIE), the reaction rate of molecules containing heavier isotopes is usually lower than the molecules containing lighter isotopes (Atkinson R., 1986; Kirillova et al., 2013; Fisseha et al., 2009). The change in reaction rate is primarily results from the greater energetic need for molecules containing heavier isotopes to reach the transition state (Nina et al., 1979). Consequently, the oxidants preferentially react with molecules with lighter isotopes (inverse kinetic isotope effect, KIE), which would result in an enrichment of ^{13}C in the residual materials and a depletion in ^{13}C of the particulate oxidation products (Rudolph et al., 2002). Therefore, organic compounds formed via secondary formation are generally depleted in ^{13}C compared with their precursors (Sakugawa and Kaplan, 1995, Fisseha et al., 2009) and this isotope depletion is demonstrated in both field measurements and laboratory studies (Pavuluri and Kawamura, 2012). For example, the studies of KIE clearly indicate that the compounds formed via the oxidation are depleted in the ^{13}C compared with their precursors during the reaction of VOCs with OH and ozone (dominant atmospheric oxidants) (Iannone et al., 2003; Rudolph et al., 2000; Anderson et al., 2004; Fisseha et al., 2009). Whereas an enrichment of ^{13}C in the particulate organic aerosol may occur in the atmospheric aging processes, such as interactions with photochemical oxidants (e.g. hydroxyl radical and ozone) during the long range transport. For instance, studies have demonstrated that the substantial enrichment of ^{13}C in the residual, aged aerosol (e.g. isoprene, a precursor of

oxalic acid (Rudolph et al., 2003)) after a long range transport. In that case, the stable carbon isotope can be used to study the sources and the atmospheric processes that contribute to the carbonaceous aerosols.".

(3) The method needs to be explained much more clearly and in more detail, including the flow rate of He, the volume of the bottle (6 mL extraction for the 20 mm diameter disc, but how much for the TOC analysis, and how much use for the δ13C-WSOC analysis, if all use for δ13C-WSOC analysis, and another one for TOC, then the results in fig 4 need be reconsider due to the maldistribution in one filter), the volume of sample extracted solution, the ratio of sample extracted solution to the oxidizing agents....

Response: According to the reviewer's advice, the method part was described in more detail and more clearly in Section 2.4 in the revised MS. And some specific information was added in both text and figures (please see the response to the minor points).

In addition, 6 mL extraction for the 20 mm diameter disc was all for the analysis of the carbon content and $\delta^{13}C$ values using Gas Bench II-IRMS. And another disc was dissolved for the analysis of TOC analyzer. The uniform distribution of the aerosol on the filter was a basic assumption in the aerosol filters analysis. In that case, the comparison of the results from the two equipment is reliable.

The volume of the sample extract was 4 mL, and 1mL oxidant solution made within 24 hours should be added in the vials. Please see Figure 1 and line 909-917 in the revised MS.

The revised Section 2.4:

2.4 Sample pretreatment

The wet oxidation method is used to covert the WSOC to CO_2 (Sharp J. H., 1973), and the resulting CO_2 can be measured by IRMS. The overview of the optimized method for measuring WSOC and $\delta^{13}C_{\text{-WSOC}}$ in the aerosols is shown in Fig. 1. The process of the pretreatment consists of 6 steps: WSOC on a 20 mm diameter disc is extracted with 6 mL mili-Q water through water-bath ultrasonic for 30 minutes (step 1-2). The WSOC extract is filtered with a 0.22 μm syringe filter to remove the particles

in step 3. 2.0 g potassium persulfate ($K_2S_2O_8$, Aladdin Industrial Corporation, Shanghai) and 100 μL phosphoric acid (85 % H_3PO_4, AR, ANPEL Laboratory Technologies Inc., Shanghai) are dissolved in 50 mL Milli-Q water to make the oxidizing solution. The oxidizing solution made within 24 h is added into the filtered WSOC extract as shown in step 4 of Fig. 1. The phosphoric acid is added to remove the inorganic carbon resolved in the solution, and the persulfate is added for the preparation to convert the organic compounds to CO_2. The vails are sealed tightly with the caps as soon as the oxidizing solution is added into the WSOC extract.

To remove the ambient CO_2 dissolved in the mixture (mixed solution of the oxidizing solution and the WSOC extract) and the atmospheric CO_2 in the headspace of the sealed sample vials, high-purity helium (Grade 5.0, 99.999 % purity) is flushed into the vials for 5 min in step 5. The aim of this step is to exclude the possible contamination from the atmospheric CO_2, and it has to be finished within 12 hours after the mixture of the WSOC extract and the oxidizing solution to avoid the loss of CO_2 produced under room temperature. High-purity helium (15-18 mL min^{-1}) is flushed under the water surface and a stainless steel tube is set for the output gas stream. The open end of this tube is submerged in Milli-Q water to prevent any backflow of atmospheric CO_2 (Fig. 1., step 5). After flushing, the vials are heated at 100 ˚C for 60 min in the sand bath pot (quartz sand, Y-2, Guoyu, China) to start the oxidation of WSOC in step 6. The heated vials are stored overnight at room temperature for condensing the moisture before the analysis on IRMS to prevent the damage to the measuring equipment.

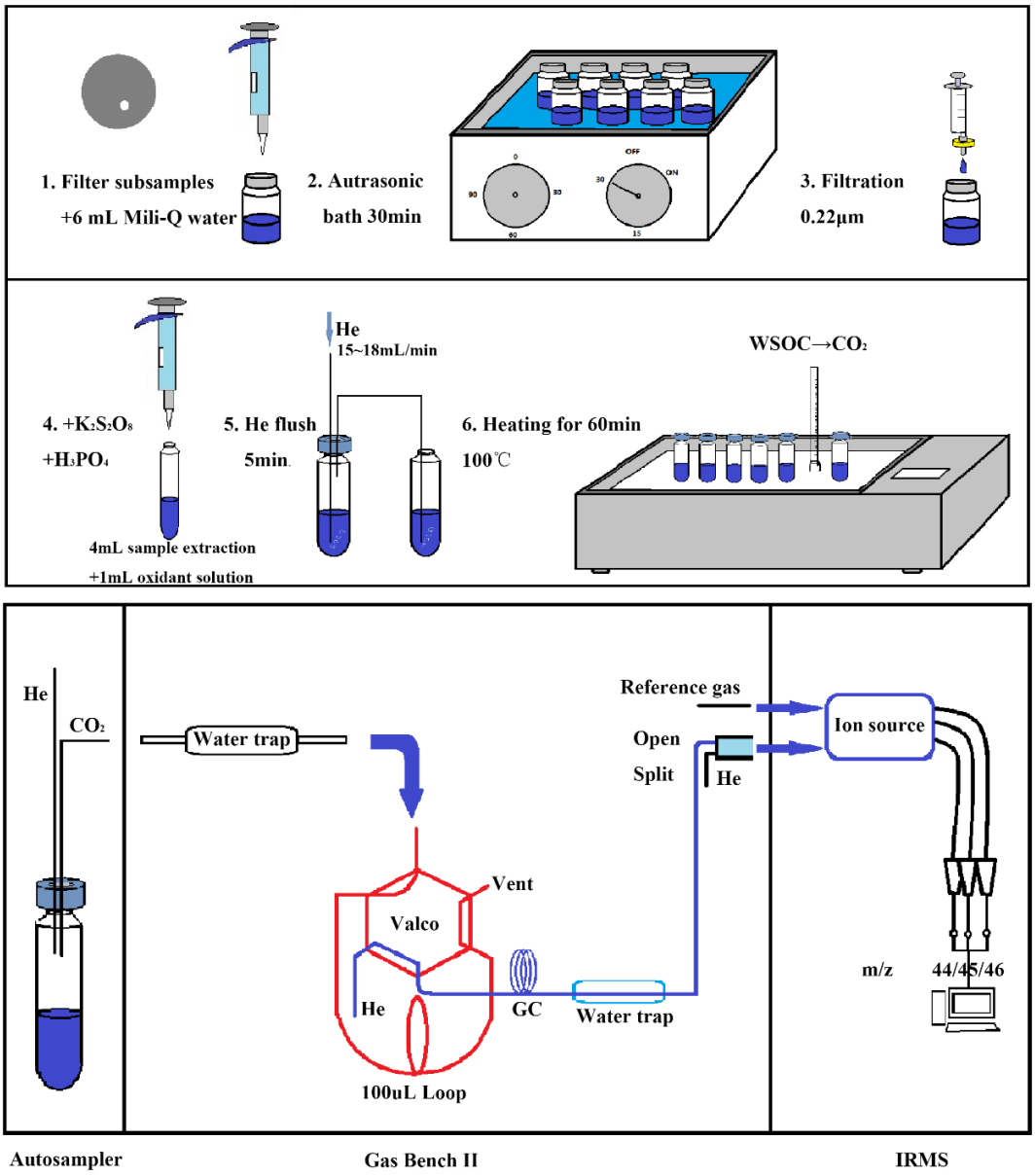

Figure 1. Schematic of the optimized method for the measurement of WSOC mass concentrations and the $\delta^{13}C_{-WSOC}$ values. (A filter disc is dissolved with 6mL Mili-Q water in a 20 mL pre-combusted glass bottle in the first step. After 30 minutes autrasonic bath, the WSOC extract is filtered with 0.22 μm syringe filter and transferred to another 20 mL pre-combusted glass bottle in step 3. 4 mL filtrate is transferred to a 12 mL pre-combusted glass vial which contains 1 mL oxidant solution (2.0g $K_2S_2O_8$ and 100 μL 85% H_3PO_4 dissolved in 50 mL Mili-Q water) in the vial in step 4. Next, the mixed solution of WSOC extract and the oxidant solution is flushed with Helium at

a flow rate of 15-18 mL min^{-1} as shown in step 5. At last, the vials are heated for 60 minutes under 100 ℃ in the sand bath pot (step 6).)

(4) adjust the 2.4 and 2.5 section after 2.1 section.

Response: Following the reviewer's suggestion, the sections were adjusted as the advised order.

(5) The conversion efficiency (removal efficiency) showed be test, which is important to quality assurance of the δ13C-WSOC results. That is because there is fractionation during the conversion processes if the conversion efficiency is low, especially during a long reaction time. The operations of removal efficiency should cover two aspects: the residual WSOC in the reaction solution and the amount of CO_2 in the bottle after heating, and compare them with the added WSOC.

Response: In order to illustrate the method that we qualify the carbon content in unknown samples, we added a new section. Please see section 3.5.1 (line 298-317) in the revised MS.

We tested the peak areas of CO_2 gas and KHP solutions (results shown in Fig. S2.). Mixture gas of CO_2 and He (0.3% mol/mol) was injected into the vials (containing carbon content from 1ug to 24 ug) for the peak area measurement. Then a standard curve of peak areas Vs carbon contents in CO_2 gas (Carbon content (μg) = Peak area (Vs) × (2.50 ± 0.08) – (0.62 ± 0.39), R^2=0.98) was set up as Fig. S2. Similarly, another standard curve of peak areas Vs carbon contents in KHP solution can be established (from the results of KHP) as well (Carbon content (μg) = Peak area (Vs) × (2.34± 0.01) – (0.86 ± 0.14), R^2=1.00), Fig. S2).

Both of the carbon contents in CO_2 gas and the KHP solution showed strongly linear correlation with peak areas. The slopes of the two linear equations were close to each other. The similarity of the two standard curves demonstrated that the WSOC extract can be oxidized to CO_2 gas containing similar amount of carbon. For example, KHP solution containing 10 ug C was expected to show peak area about 4.64 Vs, reflecting 10.8 ug C of CO_2 gas in the inflow of IRMS. Then the conversion efficiency

was roughly calculated (carbon content in CO_2 gas / input carbon content in the WSOC extract) to be 108%. This represented that almost all the WSOC extract was converted to CO_2 by the oxidation. Then we assumed the WSOC extract was completely converted to CO_2 and would show no significant isotope fractionation in our method.

The revised section 3.5.1:

3.5.1 Quantification of the carbon content

The sample peak area is proportional to the carbon content in the vial and then is used to quantify the amount of CO_2 in the inflow of IRMS. The average value of the peak areas for the last eight sample peaks is taken as the peak area of a certain sample. The first two sample peaks are excluded to avoid the effect of the residual CO_2 of the former vial. We established a carbon content standard curve (linear equation) by measuring the peak areas of CO_2 gas samples containing 1-24 μg C (Fig. S2.). It has to be noted that the gas samples containing larger carbon contents are not tested for the difficulty of injecting too much volume of CO_2/He gas. Then the amount of CO_2 oxidized from the unknown samples can be quantified with this linear equation (i.e., Carbon content (μg) = Peak area (Vs) × (2.50 ± 0.08) – (0.62 ± 0.39), R^2=0.98). The standard curve (linear equation) of the peak areas against the carbon contents in the WSOC solution (KHP solution containing 1-100 μg C) is also established (Fig. S2.). And a linear equation similar with the peak areas against CO_2 gas is obtained (i.e., Carbon content (μg) = Peak area (Vs) × (2.34± 0.01) – (0.86 ± 0.14), R^2=1.00).

Then the conversion efficiency of the WSOC extract containing 1-100 μg C can be roughly calculated as 104 ± 3 %. The high conversion efficiency demonstrates the completely conversion and the negligible isotope fractionation during the oxidation. In that case, the carbon content in the WSOC extract of unknown samples can be calculated based on the standard curve of peak areas against the carbon content in the WSOC extract. And the standard curve quantifying the carbon content has to be established with every batch of unknown samples to assure the completely conversion.

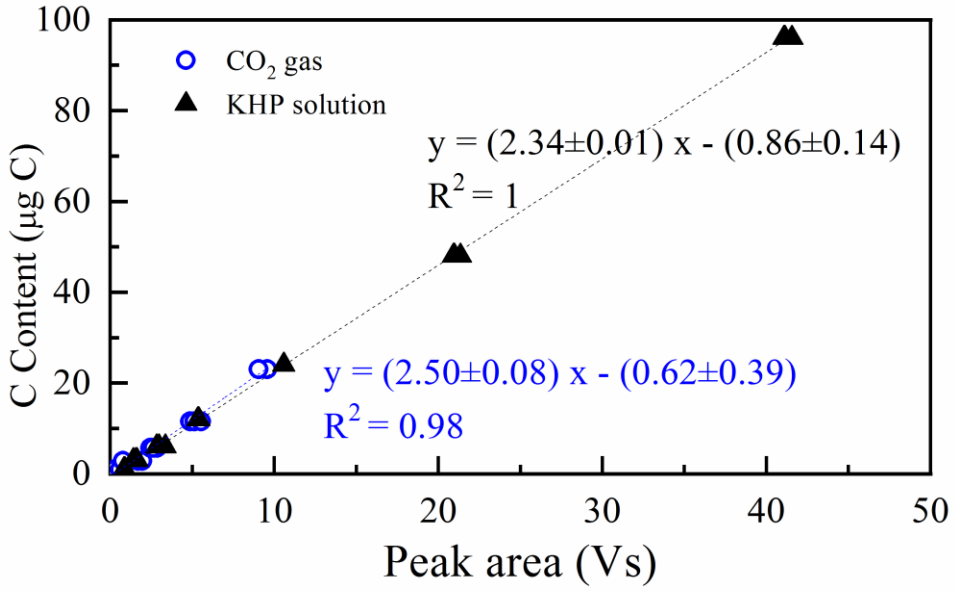

Figure S2. Standard curve to quantify the unknown samples.

(The standard curve is established by the CO_2 gas / the KHP solution and the input carbon content of the certain vials. The blue dotted line is the linear fit of the results of CO_2 gas, and the black dotted line is the linear fit of the results of KHP solution.)

(6) The IRMS method for WSOC concentration showed be present detail in the method section, rather than a single sentence like "Line 236 the peak area obtained from the measurement could represent the carbon content". If it means using the peak area represent the CO2 amounts in the inflow of IRMS? If yes, then show which peak use (10 peak total?), the gas volume in bottle and into IRMS (in the atm pressure, notice, the sample have different C content will product different amounts of CO2, and result in different pressure in the bottle), and the standard curve for the peak areaâ ˇ A ˇ TCO2 in the bottle (or the WSOC, but need do the conversion efficiency test first).

Response: Following the reviewer's suggestion, the IRMS method for WSOC concentration were described in more detail in a new section 3.5.1. Please see the response to the last comment (5), or line 298-317 in the revised MS.

The peak areas obtained from the Gas Bench II-IRMS were proportional to the carbon contents in the vials. Thus the peak areas were taken to represent the carbon content. We used the average values of the last 8 peaks to avoid the memory effect in the first two peaks. The gas volume in the bottles were the same (7 mL of headspace in the vials), and 100 µL CO_2 mixed with He was injected into the IRMS every 70 s. The standard curve of the peak areas and the carbon contents (amount of CO_2) in the vials was Carbon content (µg) = Peak area (Vs) × (2.34± 0.01) – (0.86 ± 0.14), R^2=1.00). It was added in the supporting information (S2). Please see the response to (5).

(7) How to explain the WSOC-IPMS method larger than the WSOC-TOC (fig 4)? And why some 30 µg-standard have the WSOC larger than 30 µg? Please reconsider (5) and (6)

Response: There is systematic bias between the two equipment (TOC analyzer and Gas Bench II), and the recovery of the ambient samples is 99 ±10%. In addition, data shown in Fig. 4. were the results of ambient WSOC aerosols instead of the standards. The data were obtained from Gas Bench II-IRMS (x axis) and TOC analyzer (y axis). Also, the carbon contents were calculated with the peak areas in the wet oxidation method using the Gas Bench II – IRMS. According to the recovery (97 ±6%) of this method, we regarded the WSOC conversion was complete, and the carbon content measured using this optimized method was reliable.

(8) Line 206: the explain for the 13C-WSOC increase is kinetic isotope effect (KIE). This explanation is not reasonable because the leak process is fast and driven by strong motivation, which may not result in KIE. The mixture with CO2 in ambient air (-9‰ to -7‰ seems more reasonable. In addition, I agree the leak-sample will have a low WSOC content, but not all the leak-sample have a large 13C value showed in fig 2, for example, there are one 30 µg standard sample have relatively lower WSOC content, but no significant difference between all the 30 µg samples. Please explain.

Response: We agree that the gas leak of the vials with deformed caps are fast and driven by strong motivation. But gases in the vials could also leak out through the tiny

holes purged by the stainless tube in the helium flushing step. And this kind of leak is slow and not easy to be observed.

In our opinion, atmospheric CO_2 was not a possible reason of the phenomenon we observed (lower carbon content corresponding with higher isotope composition). Atmospheric CO_2 contamination would result in higher carbon content and higher isotopic ratios according to the isotopic ratio of CO_2 in ambient air (-9‰ to -7‰). But this was not observed in our results. In addition, few procedures were processed to exclude the effect of the atmospheric CO_2 in the pretreatment (i.e., Step 4). H_3PO_4 was added in the oxidant solution to remove the atmospheric CO_2 dissolved in the WSOC extract as well (Step 5). Then the high purity helium was flushed into the vials to remove the CO_2 in ambient air in the headspace of the vials. In addition, the peak areas of the Mili-Q water (which has been processed with all the procedures in the pretreatment) tested in Section 3.1 were not detected, demonstrating negligible effect of the atmospheric CO_2 in the measurement of CO_2.

But we actually should apologize that the Fig. 2. was drawn in the wrong range of y axis which resulted in the loosing information of the dramatically high delta values corresponding with the low carbon contents. The revised graph was given below and the it could be seen in line 918 in the revised MS.

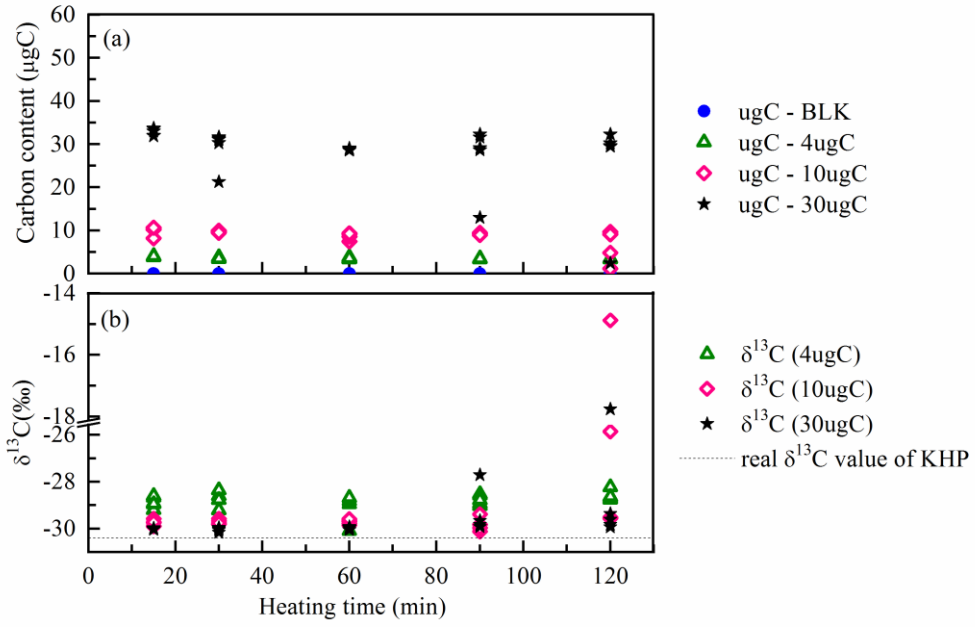

Figure 2. Carbon contents (a) and isotopic ratios (b) of KHP after different heating time.

(9) The final point bothers me is there are relatively large differences (3‰ between the monocomponent standard samples with different WSOC content. Then for the complicated real aerosol samples, during each period, the 13C-WSOC changes (3‰ with WSOC content, how to evaluate the influence of WSOC content on the 13C-WSOC. If not evaluate, the conclusion for the source or transformation processes in each episode is lack of reliability.

Response: From Fig. 3., we can see the corrected delta values of KHP (SD=0.14, n=15) and BA (SD=0.15, n=10) were stable (regardless of the carbon content in the standard) and close to the correct values ($\delta^{13}C\text{-}_{KHP}$ = -30.40‰, $\delta^{13}C\text{-}_{BA}$ = -27.17‰) tested by EA-IRMS. But the isotopic ratios of CH_6 and C_2 were more variable at small amount of carbon contents (i.e., <5μg C). We agree that the analysis of isotope compositions is not reliable if the standards show difference larger than 1‰ (SD >0.5‰) in delta values. The standard deviations of isotope results of each standard are better than 0.17 ‰ when the carbon contents are larger than 5 μg C. In that case, the detection limit of this method was 5 μg C and the results (both carbon contents and the isotopic ratios) of WSOC lower than 5 μg C were not reliable (for now). And it has to be noticed that the standard deviation of the isotope results of CH_6 was calculated without one exception (CH_6 at 6 μg C), the corrected isotopic ratio was -13.6 ‰, still about 1.5 ‰ difference with other repetitions. It was probably a wrong measurement according to the stable isotopic ratios, then it was taken as an outlier of the results.

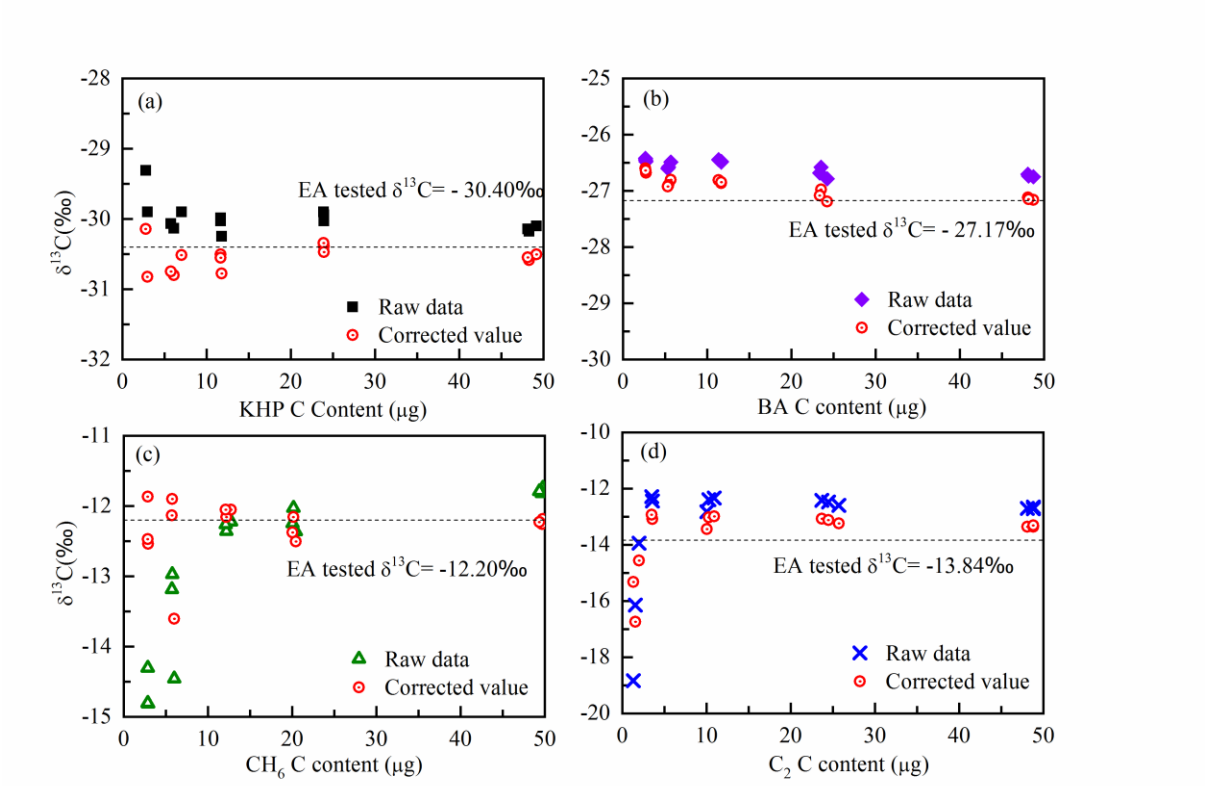

Figure 3. Isotope results before and after the two-step correction of the four standards. (a. KHP, b. BA, c. CH_6, d. C_2. Red circle with a spot represents the two-step corrected isotopic ratios; ■, ◆, △, × represent the raw data from Gas Bench II; the dotted line represents the blank corrected $\delta^{13}C$ values tested by EA)

Minor points:

Line 15-18 The difficulty for the method should be show

Response: We agree with the reviewer, and the importance and the difficulty of measuring small amount of WSOC in aerosol samples were briefly introduced in the abstract. Please see line 18-20 in the revised MS.

We added "However, the previous methods measuring the $\delta^{13}C$ values of WSOC in ambient aerosols require large amount of carbon contents as well as time-consuming and labor-intensive preprocessing."

Line 23: give the real time resolution rather than using the "High time-resolved"

Response: According to the reviewer's advice, we gave the real time solution (i.e., the aerosol samples collected every 3 hours) here. Please see line 25 in the revised MS.

The revised sentence:

However, the previous methods measuring the $\delta^{13}C$ values of WSOC in ambient aerosols require large amount of carbon contents as well as time-consuming and labor-intensive preprocessing.

Line 33: not all the dust carbonates are water-insoluble carbon

Response: We agree with the reviewer, even though a large fraction of dust carbonate is water-insoluble. So we changed the incorrect statement ("water-insoluble carbon") to "non-WSOC fraction". Please see line 35 in the revised MS.

The revised sentence:

This suggests that non-WSOC fraction in total carbon may contain ^{13}C-enriched components such as dust carbonate which is supported by the enhanced Ca^{2+} concentrations and air mass trajectories analysis.

Line 61: depleted, not enriched

Response: "Depleted" and "enriched" are relative words, for instance, marine aerosols are enriched in ^{13}C compared with C3 plant biomass burning, but depleted in ^{13}C compared with C4 plant biomass burning. So we replaced the saying of "depleted" or "enriched" with actual isotope composition to avoid the misunderstanding. Please see line 67 in the revised MS.

The revised sentence:

Marine organic aerosol sources have a carbon isotope signature of -22 ‰ to -18 ‰, (Miyazaki et al., 2011) and play an important role in the aerosols at coastal sites.

Line 84: Reference

Line 89: Reference

Response: References were added, please see line 98 and 116 in the revised MS.

Added references:

(Fisseha et al., 2006; Kirillova et al., 2010; Suto et al., 2018; Lang et al, 2012; Zhou et al., 2015).

Line 100-101: Reference, and show the representativeness for other standards.

Response: According to the reviewer's suggestion, we added the references and the representativeness for other standards. Please see line 128-131 in the revised MS.

The revised sentence:

KHP and BA are widely used as the standards of WSOC measurements (Kirillova et al., 2010) and then are used here as the WSOC test substances. Also, their isotope signatures are close to the $\delta^{13}C$ values of aerosol samples (Miyazaki et al., 2012; Fisseha et al., 2009; Suto et al., 2018).

Line 104: the exact δ for each standard, rather than the range

Response: Following the reviewer's suggestion, the exact delta values of each standard were given in both text (line 133) and Figure 3 in the revised MS.

We added "The carbon isotope composition of these four standards are: -12.20 ‰ (CH_6), -13.84 ‰ (C_2), -27.17 ‰ (BA) and -30.04 ‰ (KHP), respectively."

Line 106: give the C concentration (or the volume for the certain C mass) of the solution, and the exact magnitude, rather than the range.

Response: Following the reviewer's suggestion, the exact concentration of each standard was given in line 136-139 in the revised MS.

We added "Standards are resolved in Milli-Q water (18.2 MΩ quality) to make standard solutions of 0.25μg mL^{-1}, 0.75 μg mL^{-1}, 1.5μg mL^{-1}, 3μg mL^{-1}, 6μg mL^{-1}, 12μg mL^{-1} and 24μg mL^{-1}, which means containing carbon content of 1ug, 3ug, 6ug, 12ug, 24ug, 48ug and 96ug in 4mL standard solution to test the procedures during the pretreatment."

Line: 145 the size of the filters

Response: The size of the filter is 180×230mm, please see line 145 in the revised MS.

We added "$PM_{2.5}$ samples are collected on pre-combusted quartz-fiber filters (180×230mm) every 3 hours with a high-volume aerosol sampler (KC100, Qingdao, China) at a flow rate of 1 m^3 min^{-1}." in the revised MS.

Line142: When was the filter in 2015 measured?

Response: The WSOC on the filter collected in 2015 was measured in Nov 2016.

Line 168ïijŽthe carbon content unit?

Response: The unit of the carbon content was microgram (μg).

Line 206: the sentence is not clear.

Response: We have rewritten this sentence. Please see line 256-260 in the revised MS.

The revised sentence:

According to the kinetic isotope effect (KIE), isotope fractionation occurs during the gas leaking. The light carbon isotopes (^{12}C) are easier to escape from the vials than the heavy ones (^{13}C), thus the remaining CO_2 would be more enriched with heavy isotopes (^{13}C). In that case, lower carbon contents and higher $\delta^{13}C$ values are expected to be observed in the results of leaking vials.

Line 328-335 I agree that the fractionation during the secondary formation would result in the deplete of 13C in products (WSOC) compared to remaining substrate (the remaining VOCs), but how it can explain the explain the 13C enrichment in WSOC compared to TC?

Response: This paragraph here was explaining the secondary formed WSOC tend to be depleted in ^{13}C. Thus the ^{13}C enrichment in WSOC compared to TC **was not** mainly affected by the secondary formation of WSOC.

Line 716: Table 1 is not cited in the text

Response: We cited Table 1 in line 206 in the revised MS.

We added "To achieve this goal, the procedural blanks are analyzed to test the contamination that the reagents would introduce to the results (shown in Table 1). "

Line 702: add the size of each bottle, the volume and of solution, the flow rate of He...in Fig 1

Response: Following the reviewer's advice, we added the information in the description of Fig. 1. Please see line 909-917 in the revised MS.

The revised description of Fig.1.:

Figure 1. Schematic of the optimized method for the measurement of WSOC mass concentrations and the $\delta^{13}C_{\text{-WSOC}}$ values. (A filter disc is dissolved with 6mL Mili-Q water in a 20 mL pre-combusted glass bottle in the first step. After 30 minutes autrasonic bath, the WSOC extract is filtered with 0.22 μm syringe filter and transferred to another 20 mL pre-combusted glass bottle in step 3. 4 mL filtrate is transferred to a 12 mL pre-combusted glass vial which contains 1 mL oxidant solution (2.0g $K_2S_2O_8$ and 100 μL 85% H_3PO_4 dissolved in 50 mL Mili-Q water) in the vial in step 4. Next, the mixed solution of WSOC extract and the oxidant solution is flushed with Helium at a flow rate of 15-18 mL min^{-1} as shown in step 5. At last, the vials are heated for 60 minutes under 100 ℃ in the sand bath pot (step 6).)

Line 725: add the real δ13C-KHP in Fig 2b, as a line

Response: Following the reviewer's advice, we added the correct value of $\delta^{13}C$-KHP in Fig. 2b. as a line. Please see figure 2b. in the response to (8) or line 919 in the revised MS.

Line 728 and 738: Please unify the use of frame lines

Response: Following the reviewer's advice, we added the frame lines in Fig. 3. and 5. Please see Fig. 3. in the response to (9) or line 922 in the revised MS.

The revised Fig. 5.: line 931 in the revised MS.

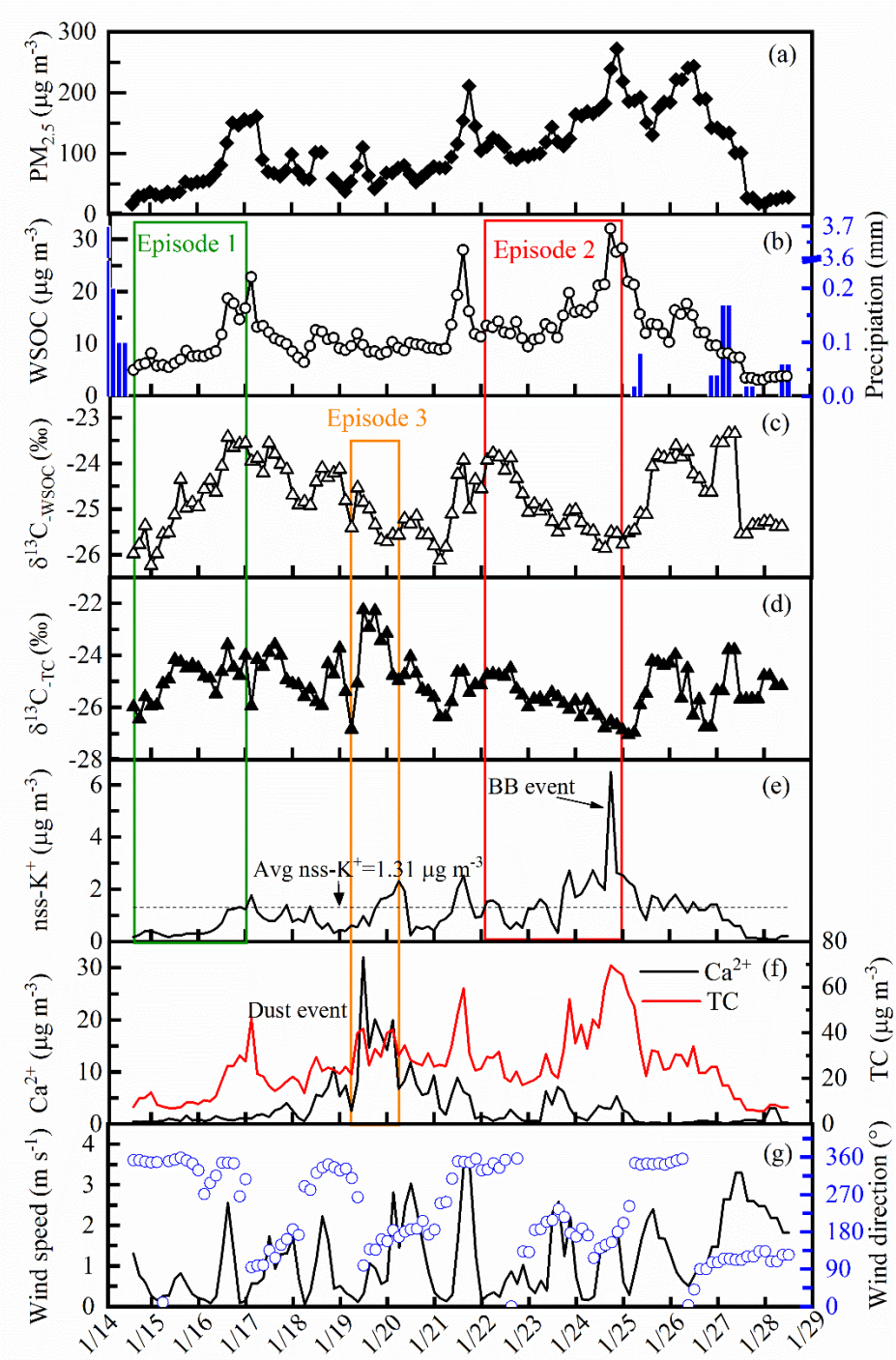

Figure 5. Time series of $PM_{2.5}$, WSOC, precipitation, $\delta^{13}C$ values, nss-K^+, Ca^{2+}, TC, wind speed and wind direction at the sampling site during the studied period. (The time period framed with the rectangles is defined as the Episode 1 (green), the Episode 2 (red) and the Episode 3 (orange). The dotted line in 5e is the average value of nss-K^+ during the studied period. The high concentration and intense increase of nss-K^+ in the

Episode 2 indicate a significant biomass burning (BB) event, and is marked with "BB event" in 5e. The similar trends of Ca^{2+} and TC suggest a dust event in the Episode 3.**)**

Line 734: add the 1:1 line and the correlation line

Response: Following the reviewer's advice, we added the 1:1 line and the correlation line as well as the linear equation in Figure 4. Please see line 927 in the revised MS.

The revised Fig.4.:

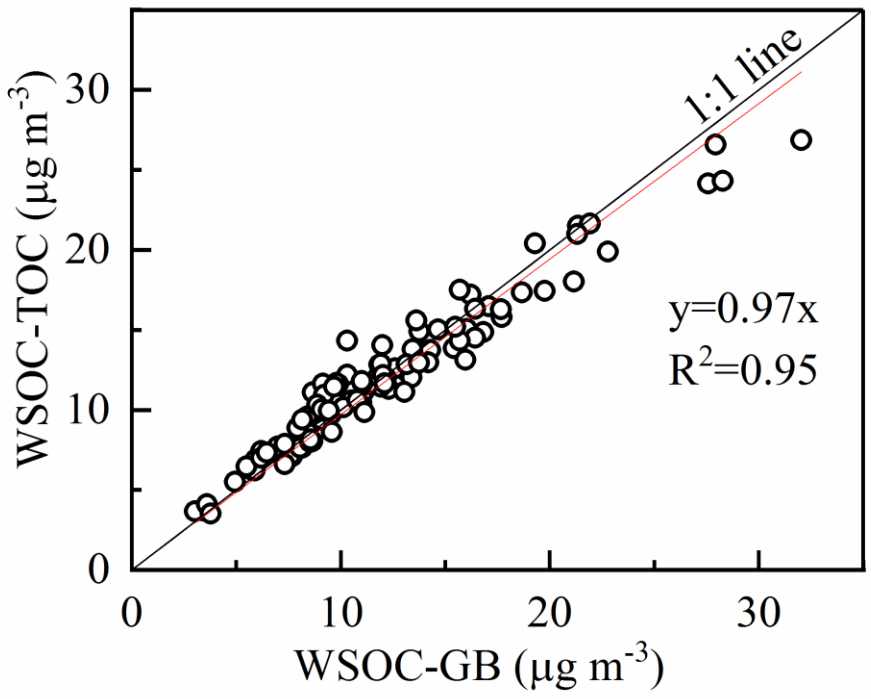

Figure 4. Correlation of WSOC mass concentrations measured with Gas Bench II - IRMS and TOC analyzer.

High time-resolved measurement of stable carbon isotope composition in water-soluble organic aerosols: method optimization and a case study during winter haze in East China

Wenqi Zhang[1,2,3], Yan-Lin Zhang[1,2,3]*, Fang Cao[1,2,3], Yankun Xiang[1,2,3], Yuanyuan Zhang[1,2,3], Mengying Bao[1,2,3], Xiaoyan Liu[1,2,3], Yu-Chi Lin[1,2,3]

1Yale–NUIST Center on Atmospheric Environment, International Joint Laboratory on Climate and Environment Change (ILCEC), Nanjing University of Information Science and Technology, Nanjing 210044, China

2Key Laboratory of Meteorological Disaster, Ministry of Education (KLME)/ Collaborative Innovation Center on Forecast and Evaluation of Meteorological Disasters (CIC-FEMD), Nanjing University of Information Science and Technology, Nanjing 210044, China

3Jiangsu Provincial Key Laboratory of Agricultural Meteorology, College of Applied Meteorology, Nanjing University of Information Science and Technology, Nanjing 210044, China

Abstract: Water soluble organic carbon (WSOC) is a significant fraction of organic carbon (OC) in atmospheric aerosols. WSOC is of great interest due to its significant effects on atmospheric chemistry, the Earth's climate and human health. Stable carbon isotope ($\delta^{13}C$) can be used to track the potential sources and investigate atmospheric processes of organic aerosols. However, the previous methods measuring the $\delta^{13}C$ values of WSOC in ambient aerosols require large amount of carbon contents as well as time-consuming and labor-intensive preprocessing. In this study, a method of simultaneously measuring the mass concentration and the $\delta^{13}C$ values of WSOC from aerosol samples is established by coupling the Gas Bench II preparation device with isotopic ratio mass spectrometry. The precision and accuracy of isotope determination is better than 0.17 ‰ and 0.5 ‰, respectively, for samples containing WSOC larger than 5 μg. This method is then applied for the aerosol samples collected every 3 hours during a severe wintertime haze period in Nanjing, East China. WSOC varies between 3-32 μg m^{-3}, whereas $\delta^{13}C_{\text{-WSOC}}$ ranges from -26.24 ‰ to -23.35 ‰. Three different episodes (e.g., namely the Episode 1, the Episode 2, the Episode 3) are identified in the sampling period, showing a different tendency of $\delta^{13}C_{\text{-WSOC}}$ with the accumulation process of WSOC aerosols. The increases in both the WSOC mass concentrations and the $\delta^{13}C_{\text{-WSOC}}$

values in the Episode 1 indicate that WSOC is subject to a substantial photochemical aging during the air mass transport. In the Episode 2, the decline of the $\delta^{13}C_{-WSOC}$ is accompanied by the increase in the WSOC mass concentrations, which is associated with regional-transported biomass burning emissions. In the Episode 3, heavier isotope (^{13}C) is exclusively enriched in total carbon (TC) compares to WSOC aerosols. This suggests that non-WSOC fraction in total carbon may contain ^{13}C-enriched components such as dust carbonate which is supported by the enhanced Ca^{2+} concentrations and air mass trajectories analysis. The present study provides a novel method to determine the stable carbon isotope composition of WSOC and it offers a great potential to better understand the source emission, the atmospheric aging and the secondary production of water soluble organic aerosols.

Key words: WSOC, stable carbon, $\delta^{13}C$, aging

1. Introduction

Water soluble organic carbon (WSOC) contributes a large fraction (9-75 %) to the organic carbon (OC) (Anderson, et al., 2008; Decesari et al., 2007; Sullivan et al., 2004) and affects substantially the global climate change and human health (Myhre, 2009; Ramanathan et al., 2001). Due to its hydrophilic nature, WSOC has a great impact on the hygroscopic properties of aerosols and promotes to increase the cloud condensation nuclei (CCN) activity (Asa-Awuku et al., 2011). WSOC is a contributor to cardiovascular and respiratory problems because it is easy to be incorporated in biological systems such as human blood and lungs (Mills et al., 2009).

WSOC can be emitted as primary organic carbon (POC) and secondary organic carbon (SOC) produced from atmospheric oxidation of volatile organic compounds (VOCs) (Sannigrahi et al., 2006; Weber et al., 2007; Zhang et al., 2018). Due to the hygroscopic property of the WSOC, the origins of POC may be from biomass burning or marine emissions. However, the SOC may stem from various sources including coal combustion, vehicle emissions, biogenic emissions, marine emissions and biomass burning (Kirillova et al., 2010, 2013; Jimenez et al., 2009; Decesari et al., 2007; Bozzetti et al., 2017b; Bozzetti et al., 2017a).

Stable carbon isotopic composition ($\delta^{13}C$) can provide valuable information to track both potential sources and atmospheric processes of carbonaceous aerosols (Rudolph, 2007; Pavuluri and Kawamura, 2012; Kirillova et al., 2013; Kirillova et al., 2014). Carbonaceous aerosols from coal combustion have an isotope signature from -24.9 ‰ to -21 ‰ (Cao et al., 2011). Particulate matter emitted from motor vehicles exhibits with isotopes from -26 ‰ to -28 ‰ (Widory, 2006), respectively. Due to the different pathways of metabolism, C3 and C4 plants exhibit significant differences of $\delta^{13}C$ (approximately -27 ‰ for C3 and -13 ‰ for C4, [Martinelli et al., 2002; Sousa Moura et al., 2008]). Laboratory studies demonstrate that there is no significant isotope fractionation (± 0.5 ‰) between the produced aerosols and the C3 plants material (Turekian et al., 1998; Currie et al., 1999; Das et al., 2010). While the C4 plants burning results in ^{13}C depletion (< 0.5 to 7.2%) in the produced aerosols (Turekian et al., 1998; Das et al., 2010). Marine organic aerosol sources have a carbon isotope signature of -22 ‰ to -18 ‰, (Miyazaki et al., 2011) and play an important role in the aerosols at coastal sites. In contrast, carbonate carbon exhibits with pretty high isotopic ratio of -0.3 ‰ (Kawamura et al., 2004), and generally shows a large proportion in dust aerosols. Thus, the isotope signatures of particulate matter emitted from these various sources may have different effect on the characteristics of $\delta^{13}C$ in ambient WSOC.

In addition, atmospheric processes like secondary formation and photochemical aging may change the constitution and properties of WSOC, as well as the stable carbon isotope of WSOC ($\delta^{13}C_{\text{-WSOC}}$). According to the kinetic isotope effect (KIE), the reaction rate of molecules containing heavier isotopes is usually lower than the molecules containing lighter isotopes (Atkinson R., 1986; Kirillova et al., 2013; Fisseha et al., 2009). The change in reaction rate is primarily results from the greater energetic need for molecules containing heavier isotopes to reach the transition state (Nina et al., 1979). Consequently, the oxidants preferentially react with molecules with lighter isotopes (inverse kinetic isotope effect, KIE), which would result in an enrichment of ^{13}C in the residual materials and a depletion in ^{13}C of the particulate oxidation products (Rudolph et al., 2002). Therefore, organic compounds formed via secondary formation are generally depleted in ^{13}C compared with their precursors (Sakugawa and Kaplan, 1995, Fisseha et al., 2009) and this isotope depletion has proven by both field measurements and laboratory studies (Pavuluri and Kawamura, 2012). For example, the studies of KIE clearly indicate that the compounds formed via the oxidation

are depleted in the ^{13}C compared with their precursors during the reaction of VOCs with OH and ozone (dominant atmospheric oxidants) (Iannone et al., 2003; Rudolph et al., 2000; Anderson et al., 2004; Fisseha et al., 2009). Whereas an enrichment of ^{13}C in the particulate organic aerosol may occur in the atmospheric aging processes, such as interactions with photochemical oxidants (e.g. hydroxyl radical and ozone) during the long range transport. For instance, studies have demonstrated that the substantial enrichment of ^{13}C in the residual, aged aerosols (e.g. isoprene, a precursor of oxalic acid (Rudolph et al., 2003) after a long range transport. In that case, the stable carbon isotope can be used to study the sources and the atmospheric processes that contribute to the carbonaceous aerosols.

Several studies report the temporal and spatial variation, complex chemical species, light absorption and thermal characteristics of WSOC, as well as its relationship with other compounds in fine particles (Wozniak et al., 2008; Wang et al., 2006; Zhang et al., 2018; Martinez et al., 2016). However, only few studies focus on the analysis of $\delta^{13}C_{\text{-WSOC}}$ (Fisseha et al., 2006; Kirillova et al., 2010; Suto et al., 2018; Lang et al, 2012; Zhou et al., 2015). This is partially due to the limited techniques to analyze the $\delta^{13}C$ signatures of WSOC in ambient aerosols, as their concentrations are usually very small. In the recent years, some efforts have been made to measure the $\delta^{13}C$ values of WSOC. Bauer et al. (1991) uses potassium persulfate to convert organic carbon in natural waters into CO_2 for $\delta^{13}C$ measurements. This wet oxidation method requires more than 0.5mM C and 1h during the pretreatment (from sample injection to the isolation of purified CO_2). Fisseha et al. (2006) boiled the oxidizing solution for 45 min to remove the organic matter and the total time required for the pretreatment (for 15 samples) is 1.5h. Kirillova et al (2010) develops a combustion method that applies the aerosol extract without filtration for isotope measurement and involves complicated processes such as the freeze-drying of the aerosol extract under vacuum for 16 h. This combustion method is the most widely used for the $\delta^{13}C$ measurements in WSOC aerosols (Kirillova et al., 2010, 2013, 2014; Miyazaki et al., 2012; Pavuluri et al, 2017). Although these methods are able to provide the $\delta^{13}C$ values of WSOC in natural waters and/or ambient aerosols, the analytical methods require either large amount of WSOC (from 100 μg C to 0.5 mM C) or time-consuming preprocessing. And some of the methods oxidize the WSOC extract without filtration and/or decarbonation in the pretreatment., which would result in higher uncertainty of the $\delta^{13}C$ results. The high detection limit

of the previous methods is difficult to determine the $\delta^{13}C_{-WSOC}$ in aerosol samples with low carbon concentrations. In that case, an easily operated method detecting the $\delta^{13}C_{-WSOC}$ values in aerosol samples with low detection limit and high precision is urgently needed. The objectives of this study are: 1) to provide an accurate, precise and easily operated method to measure the WSOC and $\delta^{13}C_{-WSOC}$ in ambient aerosol samples. 2) to apply this method for analyzing the high time resolution aerosol samples during a severe haze and discuss the potential sources and the atmospheric processes of WSOC. In addition, the concentrations of inorganic ions and air mass back trajectories coupled with MODIS fire maps are also analyzed to substantiate the results obtained from the $\delta^{13}C$ analysis.

2. Methods

2.1 Standards

Four working standards are used in this study: potassium hydrogen phthalate (KHP), benzoic acid (BA), sucrose (CH_6) and sodium oxalate (C_2). KHP and BA are widely used as the standards of WSOC measurements (Kirillova et al., 2010) and then are used here as the WSOC test substances. Also, their isotope signatures are close to the $\delta^{13}C$ values of aerosol samples (Miyazaki et al., 2012; Fisseha et al., 2009; Suto et al., 2018). Sucrose and oxalic are taken as the standards to represent the characteristics of the components in atmospheric WSOC (Fowler et al., 2018; Liang et al., 2015; Pathak et al., 2011; Pavuluri and Kawamura, 2012). The carbon isotope composition of these four standards are: -12.20 ‰ (CH_6), -13.84 ‰ (C_2), -27.17 ‰ (BA) and -30. 40 ‰ (KHP), respectively. The wide range of the delta values of the working standards is able to cover the majority of the $\delta^{13}C_{-WSOC}$ values in ambient aerosol samples. Standards are resolved in Milli-Q water (18.2 MΩ quality) to make standard solutions of 0.25μg mL^{-1}, 0.75 μg mL^{-1}, 1.5μg mL^{-1}, 3μg mL^{-1}, 6μg mL^{-1}, 12μg mL^{-1} and 24μg mL^{-1}, which means containing carbon content of 1ug, 3ug, 6ug, 12ug, 24ug, 48ug and 96ug in 4mL standard solution to test the procedures during the pretreatment.

2.2 Aerosol samples

The aerosol samples are collected during a severe haze in January (from Jan 14th to 28th) of 2015 at the suburban of Nanjing, a megacity in East China. The sampling site is located at the Agrometeorological station in the campus of the Nanjing University of Information Science and Technology. It is close to a busy traffic road and surrounded by a large number of industrial factories. $PM_{2.5}$ samples are collected on pre-combusted quartz-fiber filters (180×230mm) every 3 hours with

a high-volume aerosol sampler (KC100, Qingdao, China) at a flow rate of 1 m^3 min^{-1}. After sampling, all the filters are wrapped in the aluminum foil, sealed in air-tight polyethylene bags and stored at -26 ˚C for later analysis. A field blank is obtained by placing the blank filter in the filter holder for 10 minutes without sampling.

2.3 Chemical analysis

$PM_{2.5}$ concentrations are observed at Pukoku Environmental Supervising Station. Concentrations of total carbon (TC) and $\delta^{13}C_{-TC}$ values are analyzed with EA-IRMS (Thermo Fisher Scientific, Bremen, Germany). WSOC mass concentrations are measured with the TOC analyzer (Shimadzu). Ion concentrations are obtained from Ion Chromatograph (IC, Thermo Fisher Scientific, Bremen, Germany). Besides, the meteorological data are observed nearby the sampling site (Enivs automatic meteorological station).

2.4 Sample pretreatment

The wet oxidation method is used to covert the WSOC to CO_2 (Sharp J. H., 1973), and the resulting CO_2 can be measured by IRMS. The overview of the optimized method for measuring WSOC and $\delta^{13}C_{-WSOC}$ in the aerosols is shown in Fig. 1. The process of the pretreatment consists of 6 steps: WSOC on a 20 mm diameter disc is extracted with 6 mL mili-Q water through water-bath ultrasonic for 30 minutes (step 1-2). The WSOC extract is filtered with a 0.22 μm syringe filter to remove the particles in step 3. 2.0 g potassium persulfate ($K_2S_2O_8$, Aladdin Industrial Corporation, Shanghai) and 100 μL phosphoric acid (85 % H_3PO_4, AR, ANPEL Laboratory Technologies Inc., Shanghai) are dissolved in 50 mL Milli-Q water to make the oxidizing solution. The oxidizing solution made within 24 h is added into the filtered WSOC extract as shown in step 4 of Fig. 1. The phosphoric acid is added to remove the inorganic carbon resolved in the solution, and the persulfate is added for the preparation to convert the organic compounds to CO_2. The vails are sealed tightly with the caps as soon as the oxidizing solution is added into the WSOC extract.

To remove the ambient CO_2 dissolved in the mixture (mixed solution of the oxidizing solution and the WSOC extract) and the atmospheric CO_2 in the headspace of the sealed sample vials, high-purity helium (Grade 5.0, 99.999 % purity) is flushed into the vials for 5 min in step 5. The aim of this step is to exclude the possible contamination from the atmospheric CO_2, and it has to be finished within 12 hours after the mixture of the WSOC extract and the oxidizing solution to avoid the loss of CO_2 produced under room temperature. High-purity helium (15-18 mL min^{-1}) is flushed under

the water surface and a stainless steel tube is set for the output gas stream. The open end of this tube is submerged in Milli-Q water to prevent any backflow of atmospheric CO_2 (Fig. 1., step 5). After flushing, the vials are heated at 100 ˚C for 60 min in the sand bath pot (quartz sand, Y-2, Guoyu, China) to start the oxidation of WSOC in step 6. The heated vials are stored overnight at room temperature for condensing the moisture before the analysis on IRMS to prevent the damage to the measuring equipment.

2.5 Determination of the carbon content and stable carbon isotopic ratios

CO_2 gas produced in the headspace of the prepared sample is extracted and purified by Gas Bench II (Gas Bench II, Thermo Fisher Scientific, Bremen, Germany), and introduced into an isotope ratio mass spectrometer (IRMS) (Mat 253, Thermo Fisher Scientific, Bremen, Germany) for $\delta^{13}C_{\text{-}CO2}$ analysis. The extracted gas is purified with a Nafion water trap to remove the water vapor and then the gas is loaded into a 100 uL sample loop through an eight-port Valco valve. After 120 s loading time (the duration time from the beginning of the analysis to the first rotation of the eight port in the Gas Bench II.), the eight-port Valco valve rotates every 70 s to inject the sample gas from the loop into a GC column (Poraplot Q fused-silica cap, 25 m, 0.32 mm; Agilent Technologies). The GC column is set at 40 ˚C for the CO_2 separation from the matrix gases. The separated CO_2 is introduced into another Nafion water trap and subsequently enters into the IRMS with an open split. The CO_2 gas in each vial is detected 10 times in 15 minutes, showing 10 sample peaks after five reference peaks. The peak areas and the isotope compositions of the 10 sample peaks are given correspondingly, the results of the first two sample peaks are abandoned considering the possible memory effect of the system. The average peak area and the isotope composition of the last eight peaks is taken as the result of a certain sample determined by GB-IRMS.

3. Method optimization

The wet oxidation method is adapted from the stable isotope analysis of organic matter in ground water (Lang et al., 2012; Zhou et al., 2015). Several tests are performed to adjust the optimal conditions for measuring WSOC aerosols with relative low carbon amounts.

3.1 The carbon content in the procedural blank

In order to quantify the low concentration of WSOC in aerosols, it is critical to reduce the carbon content in the procedural blank for minimizing the detection limit of the method. To achieve this goal, the procedural blanks are analyzed to test the contamination that the reagents would

introduce to the results (shown in Table 1). The average carbon content in the procedural blank is about 0.5 μg C (corresponding with a peak area of 0.23 Vs) with a $\delta^{13}C$ value of -27.04 ± 1.28 ‰ (n=15). The carbon contents and the isotope compositions of Mili-Q water and the agents dissolved in the oxidizing solution are also determined to identify the source of contamination in the procedural blank. The peak area of Mili-Q water is not detected (Table. 1.) after going through all the processes in the pretreatment without adding any other materials, suggesting no contamination is introduced from the Mili-Q water. After that, the contamination from 85% H_3PO_4 with different purity (acid-1: analytical reagent, AR; acid-2: High Performance Liquid Chromatography, HPLC) are compared. The carbon contents in the 85% H_3PO_4 dissolved in Mili-Q water are 0.03-0.04 μg C and show no significant discrepancy between different purity.

Interestingly, the carbon content increase to 0.5-0.6 μg C after the persulfate is added, implicating that the CO_2 in the procedural blank is mainly produced from the oxidation of organic substance in the persulfate. The carbon content in HPLC grade of 85% H_3PO_4 mixed with the persulfate (0.58 - 0.63 μg C) is closed to that of AR grade (0.46 - 0.63 μg C, see table 1.). Thus, AR grade with purity of 85 % H_3PO_4 is utilized to prepare the oxidizing solution in this method. The average carbon content of the procedural blank is estimated to be 0.5 ±0.06 μg C, and the detection limit is expected to be 10 times the procedural blank (i.e. 5 μg C). The carbon content in the procedural blank of this method is much lower than that of the methods analyzing isotopes of WSOC in aquatic environment or soil (De Groot, 2004; Polissar et al., 2009; Werner et al., 1999). The smaller carbon content of the procedural blank suggests the possibility to correctly measure the WSOC and $\delta^{13}C_{\text{-WSOC}}$ of samples containing low carbon content.

3.2 Flushing methods

To avoid any contamination, the headspace of the sample vial has to be flushed with the high-purity helium to remove the CO_2 (both dissolved and gas phase). Two different flushing methods (F1 and F2) are compared here. F1 is a one-step flushing: helium is bubbled under the water surface for 5 min in a sealed vial, and the gas in the headspace is released through a stainless steel tube to the atmosphere. The open end of this tube is submerged in Milli-Q water to balance the air pressure and to prevent any backflow of the atmospheric CO_2. F2 requires two steps: the helium is first bubbled under the water surface for 5 min in an open vial to remove the dissolved CO_2 in the solution. After the vial is sealed, the helium is flushed again into the headspace for 5 min by piercing the

235 septum with a two-hole sample needle. The two holes are performed as the inlet of the helium and
236 the exit of the outflow, respectively. Since the flow rate of the inlet helium is larger than that of the
237 outflow, the headspace pressure is considered to be greater than 1atm. In that case, the most
238 noticeable difference between F1 and F2 is the air pressure of the headspace.

239 Different concentrations of working standard (KHP) are tested to compare the flushing
240 methods. The results obtained from F1 and F2 show no significant difference regardless of the
241 concentration of KHP. This represents that F1 and F2 are both able to completely remove the CO_2
242 in the vials. But it has to be noticed that F2 produces excessive air pressure in the headspace, the
243 following heating step may increase the risk of gas leak. Gas leaking during the preparation usually
244 results in the loss of carbon content and the isotope fractionation. Besides, flushing with F2 takes 5
245 more minutes for each sample compared with F1. Consequently, F1 is considered as the suitable
246 flushing method to remove CO_2 dissolved in the solution and the headspace.

247 3.3 Heating time

248 In order to assure the complete oxidation of WSOC, duration time for heating the samples is
249 tested with KHP, a widely used WSOC standard which is difficult to oxidize. Figure 2 shows the
250 carbon contents and the $\delta^{13}C$ values of KHP solutions heated from 15 min to 120 min at 100℃.
251 Some caps of the sample vials are out of shape after heating for longer time (more than 60 min),
252 suggests gas leak of the vials. High pressure can be built up in the headspace with the increase of
253 the temperature during the long time heating, especially for the vials containing more carbon
254 contents. The CO_2 gas produced in the headspace may leak through the minor holes on the septum
255 pierced by the stainless tube during the helium flushing step (step 5 in Fig 1.). According to the
256 kinetic isotope effect (KIE), isotope fractionation occurs during the gas leaking. The light carbon
257 isotopes (^{12}C) are easier to escape from the vials than the heavy ones (^{13}C), thus the remaining CO_2
258 would be more enriched with heavy isotopes (^{13}C). In that case, lower carbon contents and higher
259 $\delta^{13}C$ values are expected to be observed in the results of leaking vials. In the results of the KHP
260 standards, some of the vials containing larger amount of organic carbon are detected to have
261 extremely low carbon contents corresponding with very high isotopic ratios. For example, one of
262 the 10 μg C KHP standard is measured to be 1.2 μg C and $\delta^{13}C$ = 14.9 ‰ after 120 min of heating;
263 one of the 30 μg C KHP standard is measured to be 2.4 μg C and $\delta^{13}C$ = 17.7 ‰ after 90 min of
264 heating (Fig. 2.). The stable results (both carbon contents and the isotopes, Fig. 2.) of 4 μg C

standards are probably due to the less CO_2 gas and lower pressure produced in the headspace during the heating. Accordingly, heating time longer than 60 min increases the probability of gas leak in the measurement.

In the aspect of the isotope composition, KHP standards heated for 15min, 30min and 60 min all show stable results with similar standard deviations (from 0.51 - 0.57, see Table S1). While, the heating time of 15min and 30 min are not long enough for the complete oxidation, which is shown in lower carbon contents (Fig. 2.). Therefore, heating for 60 min at 100℃ is found to be the most suitable to produce constant results without gas leak and isotope fractionation.

3.4 Waiting time and instrument settings

The waiting time of the mixture (the aerosol extract and the oxidizing solution) between step 4 and 5 in Fig. 1. is tested to prevent the CO_2 loss during the flushing. Some of the compounds in aerosol samples could be oxidized at room temperature. The CO_2 generated from the mixture before heating could be lost during the flushing step (Sharp, 1973). The ambient sample is tested to detect the room - temperature - oxidized CO_2 (Fig. S1.). Replicates of the ambient aerosol extract (from one filter) are mixed with the oxidizing solution, and the mixtures of the aerosol extract and the oxidizing solution are flushed with He to exclude the effect of CO_2 (both in the headspace and in the mixture) as soon as possible. After flushing, the mixtures are stored at room temperature from 1 to 31 hours before analysis without heating. The carbon contents produced in the mixtures that stored less than 12 h before analysis is smaller than 0.02 μg, which contributes to ~ 7% to the carbon content in the procedural blank (0.5μg C). But when the waiting time is extended to 31 h, up to 2.3 μg C (about 5 times of the procedural blank) is oxidized into CO_2. The room - temperature - oxidized CO_2 produced during the waiting time would be flushed out by the He in the later procedure and then would result in significant isotope fractionation in the delta results. Therefore, the mixture should be flushed with He within 12 h to avoid the CO_2 loss and isotope fractionation.

In addition, various combinations of shorter loading times (30-90 s) and/or fewer sample peaks (i.e. 5 sample peaks) are tested with reference gas (CO_2 mixed with He) to shorten the analysis in the system. However, the amount of CO_2 in the reference gas detected by the mass spectrometry is about 2 μg C lower compared the results obtained with longer loading times and more sample peaks. And there is a decrease of isotope value (~ 0.4 ‰) as well when the loading time is shorter or the

sample peaks are less than 10. Thus, 120 s loading time and 10 sample peaks are necessary for the precise results, and the standard deviation is < 0.03 ‰ for the 10 sample peaks within a run.

3.5 Calibration of the results

3.5.1 Quantification of the carbon content

The sample peak area is proportional to the carbon content in the vial and then is used to quantify the amount of CO_2 in the inflow of IRMS. The average value of the peak areas for the last eight sample peaks is taken as the peak area of a certain sample. The first two sample peaks are excluded to avoid the effect of the residual CO_2 of the former vial. We established a carbon content standard curve (linear equation) by measuring the peak areas of CO_2 gas samples containing 1-24 μg C (Fig. S2.). It has to be noted that the gas samples containing larger carbon contents are not tested for the difficulty of injecting too much volume of CO_2/He gas. Then the amount of CO_2 oxidized from the unknown samples can be quantified with this linear equation (i.e., Carbon content (μg) = Peak area (Vs) × (2.50 ± 0.08) – (0.62 ± 0.39), R^2=0.98). The standard curve (linear equation) of the peak areas against the carbon contents in the WSOC solution (KHP solution containing 1-100 μg C) is also established (Fig. S2.). And a linear equation similar with the peak areas against CO_2 gas is obtained (i.e., Carbon content (μg) = Peak area (Vs) × (2.34± 0.01) – (0.86± 0.14), R^2=1.00).

Then the conversion efficiency of the WSOC extract containing 1-100 μg C can be roughly calculated as 104 ± 3 %. The high conversion efficiency demonstrates the completely conversion and the negligible isotope fractionation during the oxidation. In that case, the carbon content in the WSOC extract of unknown samples can be calculated based on the standard curve of peak areas against the carbon content in the WSOC extract. And the standard curve quantifying the carbon content has to be established with every batch of unknown samples to assure the completely conversion.

3.5.2 Blank correction

The blank contribution to the WSOC mass concentrations and the $\delta^{13}C_{-WSOC}$ values are evaluated with the peak area and the isotope value of the procedural blank. The peak area (average value of the last eight peaks) from the measurement is proportional to the carbon content in the vial and then is taken to represent the CO_2 amounts in the inflow of IRMS. The procedural blank can be corrected according to the mass balance as follows.

$$\delta^{13}C_{meas} \times A_{meas} = \delta^{13}C_{corr} \times (A_{meas} - A_{blk}) + \delta^{13}C_{blk} \times A_{blk} \quad (1)$$

Where $\delta^{13}C_{corr}$, $\delta^{13}C_{meas}$ and $\delta^{13}C_{blk}$ are the blank-corrected $\delta^{13}C$, the measured $\delta^{13}C$ of the samples and the $\delta^{13}C$ of the procedural blank, respectively. A_{meas} and A_{blk} denote the peak areas of the samples and the blank, correspondingly.

In order to calibrate the contribution of the procedural blank to the isotope results, A_{blk} and $\delta^{13}C_{blk}$ are calculated with an indirect method (Polissar et al., 2009). KHP ($\delta^{13}C$= -30. 40 ‰) and CH_6 ($\delta^{13}C$= -12.20 ‰) with various concentrations are measured to calculate A_{blk} and $\delta^{13}C_{blk}$. The wide range of their isotopes can basically cover the $\delta^{13}C_{-WSOC}$ values in most ambient aerosol samples. According to Eq. (1), $\delta^{13}C_{meas}$ can be written as the following:

$$\delta^{13}C_{meas} = \delta^{13}C_{corr} + A_{blk}(\delta^{13}C_{blk} - \delta^{13}C_{corr})/A_{meas} \quad (2)$$

According to Eq. (2), there is a linear relationship of the $\delta^{13}C_{meas}$ values and the reciprocal of peak areas ($1/A_{meas}$). Based on the keeling plot theory, linear equations of the $\delta^{13}C_{meas}$ values and $1/A_{meas}$ for the two standards can be set up separately (e.g., $\delta^{13}C$ and $1/A_{meas}$ values obtained from the measurement of CH_6 and their linear relationship are shown in Fig.S3.). The slopes (k1 and k2) and the intercepts (b1 and b2) of this liner relationship can be expressed with $\delta^{13}C_{blk}$, A_{blk} and $\delta^{13}C_{corr}$ as follows.

$$k_1 = A_{blk} \times (\delta^{13}C_{blk} - \delta^{13}C_{corr-std1})$$
$$k_2 = A_{blk} \times (\delta^{13}C_{blk} - \delta^{13}C_{corr-std2}) \quad (3)$$

$$b_1 = \delta^{13}C_{corr-std1}$$
$$b_2 = \delta^{13}C_{corr-std2} \quad (4)$$

Thus, A_b and $\delta^{13}C_b$ can be calculated as follows:

$$\delta^{13}C_{blk} = (k_2 \times b_1 - k_1 \times b_2)/(k_2 - k_1) \quad (5)$$

$$A_{blk} = (k_2 - k_1)/(b_1 - b_2) \quad (6)$$

Thus, the blank contribution is able to be calibrated with the equation below:

$$\delta^{13}C_{corr} = (\delta^{13}C_{meas} \times A_{meas} - \delta^{13}C_{blk} \times A_{blk})/(A_{meas} - A_{blk}) \quad (7)$$

For example, $\delta^{13}C_{blk}$ and A_{blk} are calculated to be -27.43‰ and 0.3Vs (~0.5 μg C) based on the results of KHP and CH_6 (shown in Fig. 3.). The carbon content in the procedural blank contributes to 1 – 10% carbon content of an ambient aerosol sample. Although the $\delta^{13}C_{blk}$ and A_{blk} are not strongly varied values, they need to be measured before every batch of the ambient samples to assure the stable status of the system (IRMS) and the proper processes during the pretreatment.

3.5.3 Calibration of isotope results

In order to calibrate the isotope results, four working standards (KHP, BA, CH_6 and C_2) containing different carbon contents are measured with EA-IRMS and Gas Bench II-IRMS. The standards measured with EA are combusted at 1000℃ to convert the organic materials into CO_2 for the measurement in IRMS without pretreatment. More than 10 repetitions of each standard are measured in this way, the average delta values (after blank correction) of each standard are defined as correct values here. On the other hand, the average isotope compositions (after blank correction) of 10 repetitions obtained from the wet oxidation method (determined with Gas Bench II) are defined as measured values. Thus the calibration curve can be established on the basis of the measured values and the correct values (Fig. S4.). For instance, the isotope results can be calibrated as follows:

$$\delta^{13}C_{cali} = k \times \delta^{13}C_{blk-corr} + b \quad (8)$$

$\delta^{13}C_{cali}$ is the isotope composition after the isotope calibration, $\delta^{13}C_{blk\text{-}corr}$ is the blank corrected isotope composition determined with Gas Bench II, k and b are the slope and the intercept obtained from the calibration curve. Similar with the blank correction, the isotope calibration curve needs to be established with each batch of the ambient samples to assure the stable status of the IRMS and the proper processes during the pretreatment.

In this way, the isotope results can be calibrated, the raw data and the isotope composition after the blank correction and the isotope calibration determined with Gas Bench II are compared in Fig. 3. The correct values of standard carbon isotopes are plotted in Fig. 3. as well. The isotope results after two steps of correction (the blank correction and the calibration of isotope results) are closer to the correct values (isotopes measured with EA) and the blank contribution are drastically eliminated. But as for the standards containing carbon content smaller than 5 μg C, the contribution of the procedural blank (with an isotope ratio about -27.43‰) is still significant. According to the isotope variation of the ambient aerosols, the analysis of isotope compositions is not reliable if the repetitions of the standards show difference larger than 1‰ (SD > 0.5 ‰). After correction, the standard deviations of isotope results of each standard are better than 0.17 ‰ (regardless of the carbon content of a certain standard) when the carbon contents are larger than 5 μg C. In that case, the detection limit of this method is 5 μg C and the results (both carbon contents and the isotopic ratios) of WSOC lower than 5 μg C were not reliable.)

3.6 QA/QC procedure

A batch of working standards with different carbon contents are measured to evaluate the optimized method in this study (data shown in Fig. 3.). The quality of the unknown samples is assured with a standard curve established with the peak areas and the corresponding input carbon contents of WSOC extract (e.g. in Fig. S2.). The conversion efficiency of the WSOC oxidation is 104 ±3% . The average recovery of the working standards and the ambient samples are tested to be 97 ± 6 % and 99 ± 10 %, respectively. The conversion efficiency and the recoveries suggest completely oxidation of WSOC extract without significant isotope fractionation in the pretreatment. The blank contribution is evaluated with the peak area and the isotopic ratio, these values are calculated with the indirect method introduced in Sect. 3.5.2. According to the carbon content (0.3 - 0.5 μg C) and the isotope composition (~ -27.43 ‰) of the procedural blank, the WSOC detection limit of this method is 5 μgC, 10 times of the carbon content in the procedural blank. The blank corrected isotope compositions should be calibrated again with the calibration curve as described in Sect. 3.5.3 to obtain the isotopic ratios of the unknown samples.

In order to obtain the carbon contents and the corrected isotope compositions of the unknown samples, at least two kinds of standards need to be measured before every batch of the unknown samples. The range of the carbon contents and the isotope compositions of the standards are required to cover the range of WSOC and $\delta^{13}C_{\text{-WSOC}}$ in the ambient samples, e.g. KHP, BA and CH_6. Hence, the concentration standard curve, the linear equations for the blank correction and the isotope calibration curve are able to be established according to the results of the standards. Besides, one standard should be measured after every 10 unknown samples to assure the stable status of the equipment.

As for the isotope measurement, the precision of the last eight sample peaks is < 0.15 ‰ within a run for standards containing more than 1 μg C; between runs, the deviation of the standards with different carbon contents (> 5 μg C, n ≥ 10) is < 0.17 ‰. The accuracy is estimated to be better than 0.5 ‰ by comparing the calibrated $\delta^{13}C$ results from Gas Bench II and the blank corrected isotopic ratios from EA. Isotope results tested by Gas Bench II is slightly lower compared to the results of EA. The ambient aerosol filters are tested repeatedly to evaluate the reproducibility of the ambient samples as well. The standard deviation of the WSOC concentrations and the isotope results of the repeated ambient samples are 0.25 ± 0.04 μg C (n≥3) and 0.14 ± 0.07 ‰ (n≥3), respectively.

To conclude, the presented method is considered to be precise and accurate to detect the low abundance of WSOC as well as isotopes in aerosol samples.

To test the applicability of this method measuring the atmospheric WSOC, the ambient aerosol samples collected in Nanjing are analyzed. And the WSOC concentrations are measured with TOC analyzer (Shimadzu) for comparison. Figure 4. shows the scattered plot of WSOC concentrations measured with the two peripherals (TOC analyzer and Gas Bench II-IRMS). The strong correlation (R^2 = 0.95, p<0.01) and the slope (0.97) demonstrate the reliability of measuring WSOC with the presented method. It suggests complete oxidation of WSOC in aerosol samples, which means no significant carbon isotope fractionation happens during the preparation. Moreover, the $\delta^{13}C_{\text{-WSOC}}$ values (between -26.24 ‰ to -23.35 ‰) of ambient aerosols are close to the published data (from -26.5 ‰ to -17.5 ‰) (Kirillova et al., 2013; Kirillova et al., 2014). In that case, the $\delta^{13}C$ values resulted from this method are considered to be effective for ambient WSOC.

4. Sources and atmospheric processes of WSOC

4.1 Temporal variation

Time series of $PM_{2.5}$, $\delta^{13}C$ values, chemical tracers and meteorological data observed at the sampling site during the studied period are illustrated in Fig. 5. WSOC ranges from 3.0 to 32.0 μg m^{-3}, occupying 49 ± 10 % of total carbon in $PM_{2.5}$. The stable carbon isotopes of WSOC and TC vary between -26.24 ‰ to -23.35 ‰ and -26.83 ‰ to -22.25 ‰, respectively. $\delta^{13}C$ values shift over 2 ‰ in 24 hours, and over 1 ‰ in 3 hours, which is not able to be captured in lower time resolution samples (e.g., 12h or 24h). In that case, this data set can be interpreted with more detailed information about the WSOC sources and the atmospheric processes. Biomass burning tracer (nss-K^+), dust tracer (Ca^{2+}), MODIS fire spots and air mass trajectories are analyzed to investigate the potential sources of WSOC. Nss-K^+ is used as a proxy of biomass burning (Zhang et al., 2013). Nss-K^+ concentrations are evaluated from Na^+ concentrations in the samples according to their respective ratios (K^+/Na^+=0.037 *w/w*) in seawater (Osada et. al., 2008).

$$\text{nss} - K^+ = [K^+] - 0.037 \cdot [Na^+] \quad (9)$$

where $[K^+]$ and $[Na^+]$ are the total mass concentrations of K^+ and Na^+ of the aerosol samples. The concentration of nss-K^+ ranges from 0.16 to 6.70 μg m^{-3} with an average of 1.31 μg m^{-3}. The high concentrations and the intense increase in Jan 24th indicate a significant biomass burning event and will be discussed later.

As shown in Fig. 5., $\delta^{13}C_{\text{-TC}}$ and $\delta^{13}C_{\text{-WSOC}}$ show similar pattern during the sampling period. In general, $\delta^{13}C_{\text{-TC}}$ is slightly lower than $\delta^{13}C_{\text{-WSOC,}}$ and the trend is also observed elsewhere (Fisseha et al., 2009). The difference is related to the sources and the atmospheric processes during the formation and transformation of carbonaceous particles in the atmosphere. The C4 plants biomass burning and the marine organic materials are the sources with relatively enriched ^{13}C. Smith and Epstein (1971) suggest that C4 plants have a mean $\delta^{13}C$ isotope signature of -13 ‰. And the isotope composition of carbon emitted from phytoplankton, an example of primary marine aerosol, is about -22 ‰ to -18 ‰ (Miyazaki et al., 2011). However, January is not a specific time period for the growing or combustion of C4 plants in East China, indicating small possibility of C4 plants biomass burning as a major source of WSOC aerosols. In addition, both WSOC and non-WSOC components can be emitted from biomass burning, thus the C4 plants combustion would generally result in the enrichment of ^{13}C in both TC and WSOC. The air parcel transported from marine areas normally has little effect on the aerosols during winter in Nanjing (Qin et al., 2016), suggesting the negligible contribution of marine emissions to WSOC during the sampling period. Therefore, the WSOC sources with higher isotope signatures (compared with non-WSOC sources) are not able to explain the higher values of $\delta^{13}C_{\text{-WSOC}}$ over $\delta^{13}C_{\text{-TC}}$.

Apart from the sources, the secondary formation (Hecobian et al., 2010; Jimenez et al., 2009; Saarikoski et al., 2008) of WSOC is reported to affect the isotope compositions. Precursors like VOCs can be oxidized with the hydroxyl radicals and ozone to produce WSOC in the atmosphere (Pathak et al., 2011). Laboratory and field studies demonstrate that the lighter isotopes have the priority to be oxidized and produce particulates with lower isotopic ratios. For example, the oxidation of VOCs in the atmosphere would result in the ^{13}C depletion in the products and the ^{13}C enrichment in the residual VOCs (Rudolph et al., 2002). In other words, the secondary formation tends to lower the $\delta^{13}C$ value of ambient WSOC, thus the secondary formation could not explain the ^{13}C enrichment in WSOC compared to TC.

Studies demonstrate that the photochemical aging process during the long range transport causes significant enrichment in ^{13}C. (Aggarwal and Kawamura, 2008; G. Wang et al., 2010). The isotope fractionation is up to 3 ‰ - 7 ‰ of the residual during the photolysis of oxalic acid, a dominant species in WSOC aerosols (Pathak et al., 2011). Due to the hydrophilic property, WSOC is associated with the aerosol aging processes. WSOC/OC ratio is normally considered to represent

471 the aging status of aerosol samples (Agarwal et al., 2010; Pathak et al., 2011), it increases with the
472 photochemical aging process. The ratio of WSOC/OC is 0.67 ±0.12 (Fig. S5.) in this study, which
473 is higher than the aged aerosols with WSOC/OC = 0.41 reported elsewhere (Huang et al., 2012).
474 The high ratio of WSOC/OC indicates aged aerosols during the sampling period. Thus the
475 photochemical aging process could partially explain the reason of higher values of $\delta^{13}C_{\text{-WSOC}}$
476 (compared with $\delta^{13}C_{\text{-TC}}$).

477 According to the principle of mass balance, ^{13}C depleted sources of non-WSOC can also result
478 in the depletion of ^{13}C in TC. TC is consist of OC, EC and carbonate carbon (CC) (Huang et al.,
479 2006), and OC can be divided into WSOC and water insoluble OC (WIOC) according to the
480 hydrophilic character (Eq. 10). In most circumstances, CC is negligible to the amount of TC in $PM_{2.5}$
481 (Huang et al., 2006; Ten Brink et al., 2004), thus non-WSOC component could be presented as Eq.
482 11.

483 $$\mathrm{TC} = \mathrm{OC} + \mathrm{EC} + \mathrm{CC} = \mathrm{WSOC} + \mathrm{WIOC} + \mathrm{EC} + \mathrm{CC} \quad (10)$$

484 $$\mathrm{TC} - \mathrm{WSOC} = \mathrm{WIOC} + \mathrm{EC} \quad (11)$$

485 WIOC and EC are generally originated from primary emissions (Park et al., 2013; Y. L. Zhang
486 et al., 2014), and the $\delta^{13}C$ values are better representing their sources. In that case, the ^{13}C depleted
487 source which only contributes to non-WSOC components, such as WIOC emitted from the
488 vegetation, is likely to be another reason of $\delta^{13}C_{\text{-TC}}$ depletion during the sampling period.

489 4.2 Three episodes

490 During the sampling period, three significant haze events (e.g., namely the Episode 1, the
491 Episode 2, the Episode 3) are observed in Nanjing. These 3 episodes show different tendencies of
492 $\delta^{13}C_{\text{-WSOC}}$ variation during the accumulation of WSOC aerosols (see Fig. 5.). The Episode 1 and 2
493 are compared here due to the distinct $\delta^{13}C_{\text{-WSOC}}$ trends with WSOC accumulation. In the Episode 3,
494 ^{13}C is found to be enriched in TC compared to WSOC ($\delta^{13}C_{\text{-WSOC}} < \delta^{13}C_{\text{-TC}}$, $p<0.01$), in contrast to
495 the trend of isotope compositions during other periods ($\delta^{13}C_{\text{-WSOC}} > \delta^{13}C_{\text{-TC}}$, $p<0.01$).

496 4.2.1 The Episode 1

497 As for the Episode 1, the $\delta^{13}C_{\text{-WSOC}}$ values increase with the mass concentrations of WSOC (r
498 = 0.84, $p < 0.001$, see Fig. 6d.), indicating the sampling site is impacted by ^{13}C enriched WSOC
499 sources and/or photochemical aged aerosols. As shown in Fig. 6a., air mass trajectories of WSOC
500 with higher $\delta^{13}C_{\text{-WSOC}}$ values (>24‰) are originated mainly from northern China, and the northerly

wind prevails at this site (Fig. 5g.). During the long-range transport, the studied WSOC mass concentration increases with the ^{13}C enrichment of WSOC due to the isotope fractionation in the photochemical aging process. This is supported by the increasing ratio of WSOC/OC (from 0.73 to 0.91) in the Episode 1 (Fig. S5.).

According to the higher isotopes ($\delta^{13}C_{\text{-WSOC}} > -24$ ‰) and the corresponding trajectories (Fig. 6a.), C4 plants biomass burning ($\delta^{13}C \sim -12$‰, [Martinelli et al., 2002; Sousa Moura et al., 2008]) and coal combustion ($\delta^{13}C \sim -24.9$ ‰ to -21 ‰, [Cao et al., 2011]) are considered to be possible sources of WSOC. Nss-K^+ is largely originated from plants combustion (Zhang et al., 2013), and is analyzed as a proxy of biomass burning. However, during this period the nss-K^+ level (0.56 ± 0.41 μg m^{-3}) is not significantly increased and is generally lower than the average value (1.3 μg m^{-3}, Fig.5e), indicating that the C4 plants biomass burning is not a major source of WSOC. Besides, the main crops growing in northern China are mainly C3 plants such as wheat and rice instead of C4 plants during the sampling period (Chen et al., 2004). And the biomass burning contribution of C3 plants would even lower the $\delta^{13}C$ values of WSOC. What's more, there are only few MODIS fire spots along with the trajectories from northern China (Fig. 6a.). In that case, open field biomass burning is not considered as a major source of WSOC at the sampling site during the Episode 1.

Furthermore, the WSOC mass concentrations and the $\delta^{13}C_{\text{-WSOC}}$ values decrease synchronously with the change of the wind direction (from north to southeast) after the Episode 1. The southeast wind breaks the continuous transport of WSOC from northern China. And the relatively lower $\delta^{13}C_{\text{-WSOC}}$ values are then observed, suggesting a regional isotope signal of WSOC without the substantial aging. Besides, the WSOC/OC declines obviously with the isotope after the Episode 1 (Fig. S5.), indicating less contribution of aged aerosols to the sampling site. Therefore, the elevated $\delta^{13}C_{\text{-WSOC}}$ values with the increased WSOC mass concentrations in the Episode 1 are mainly affected by the aged aerosols transported from northern China.

4.2.2 The Episode 2

The $\delta^{13}C_{\text{-WSOC}}$ values show an opposite trend with WSOC mass concentrations ($r = -0.54$, $p < 0.01$, see Fig. 6e.) in the Episode 2. At the beginning of the Episode 2 (Jan 22nd), the sampling site is mainly affected by the air mass from the north of Nanjing, and the WSOC displays with relatively higher $\delta^{13}C_{\text{-WSOC}}$ values at the same time (Fig. 6b). After Jan 22nd, the shift of the wind direction and the air mass trajectories are well corresponded with the decline of the $\delta^{13}C_{\text{-WSOC}}$ values (Fig.

6b.). The large amount of fire spots in the potential source regions suggests the significant impact of open field biomass burning. It should be noted that the stable carbon isotope composition of C3 plants combustion is relatively low (i.e., $\delta^{13}C$~ -27‰, [Martinelli et al., 2002; Sousa Moura et al., 2008]). The $\delta^{13}C_{\text{-WSOC}}$ values decrease and the WSOC mass concentrations peak to the maximum when the air mass travels throughout the regions with a great many hot spots. The concentration of nss-K^+ has a positive correlation with WSOC concentration ($r = 0.82$, $p < 0.001$) and a negative correlation with $\delta^{13}C_{\text{-WSOC}}$ ($r = -0.45$, $p < 0.05$) during the Episode 2. And the concentration of nss-K^+ increases up to 6.7 μg m^{-3}, about 7 times of the average value, indicating a significant biomass burning contribution (Fig. 5e). The decrease of the $\delta^{13}C_{\text{-WSOC}}$ values and the increase of the biomass burning tracers (i.e., nss-K^+) suggest that the biomass burning emission is a major contribution of WSOC aerosols. Also, the WSOC/OC ratio declines from 0.88 to 0.53 (Fig. S5.), indicating that the increased WSOC is rather from fresh biomass-burning aerosols without a substantial aging process.

4.2.3 The Episode 3

The ^{13}C is clearly enriched ($p<0.01$) in TC (-23.5 ± 0.43 ‰) compared to WSOC (-25.17 ± 1.08 ‰) during the Episode 3 (see Fig. 6f.). This might be related with a ^{13}C-enriched source and/or the aging process of non-WSOC fraction in TC. Non-WSOC fraction is mainly consist of WIOC, EC and carbonate carbon (CC). Among these carbonaceous species, carbonate carbon (CC) exhibits with much higher $\delta^{13}C$ values than EC and OC (Kawamura et al., 2004). CC could be a significant fraction of dust aerosols, even though it is a very small part of TC in $PM_{2.5}$ in most cases.

To study the dust contribution in the Episode 3, Ca^{2+} is determined as an indicator of dust (Huang et al., 2010; Jankowski et al., 2008). Ca^{2+} and TC show similar patterns ($R^2 = 0.84$, $p < 0.01$), indicating dust origins in this period. The argument is also supported by the 48-h backward trajectory analysis (Fig. 6c.). It shows that the air mass is mainly originated from a semi-arid region, Mongolia. The photochemical aging of dust aerosols during the long-range transport from Mongolia to Nanjing could possibly promotes the ^{13}C enrichment. For short, the enrichment of ^{13}C in TC over WSOC is due to a dust event transported to the studied site.

According to the mass balance, the isotopic ratio of TC affected by CC in the dust aerosols can be expressed as follows:

$$\delta^{13}C_{-TC} = f_{cc} \times \delta^{13}C_{-CC} + (1 - f_{cc}) \times \delta^{13}C_{-NC} \quad (12)$$

where the $\delta^{13}C_{-TC}$, $\delta^{13}C_{-CC}$ and $\delta^{13}C_{-NC}$ are the measured stable carbon isotope of TC, the isotopic ratio of CC in dust aerosols and the isotope composition of non-CC fractions. The f_{cc} represents the CC contribution to TC. The CC contribution during the Episode 3 is roughly estimated based on a few assumptions: 1) the increase of TC and $\delta^{13}C_{-TC}$ is only affected by the dust origin, 2) the average value of $\delta^{13}C_{-TC}$ (-25 ‰) during the studied period (except the Episode 3) is taken as the value of $\delta^{13}C_{-NC}$, 3) $\delta^{13}C_{-CC}$ = 0.3 ‰ in dust sources (Kawamura et al., 2004). With these considerations, CC contribution is estimated to contribute up to 10% to TC according to the Eq. 12.

5. Conclusions

An optimized method for the determination of WSOC mass concentrations and $\delta^{13}C_{-WSOC}$ values in aerosol samples with Gas Bench II - IRMS is presented. A two-step correction is applied to correct the blank contribution and to calibrate the isotope results. The procedural blank is estimated to be 0.5 μgC with isotope composition of -27.43 ‰. The detection limit is demonstrated to be 5 μgC according to the measurement of working standards with various carbon contents. The method yields a high recovery of the standards (97 ± 6 %) and ambient samples (99 ± 10 %). According to the high recoveries, the isotope fractionation during the pretreatment is tend to be negligible. The precision and the accuracy is better than 0.17 ‰ and 0.5 ‰, separately. WSOC concentrations determined with this optimized method is consistent (R^2 = 0.95) with the results of the TOC analyzer. Compared with the previous methods, the optimized method presented in this study is more precise and accurate, and requires less time-consuming pretreatment.

The presented method is then applied to analyze the $\delta^{13}C_{-WSOC}$ of the high time resolution aerosol samples collected during a severe winter haze in East China. WSOC ranged from 3.0 μg m^{-3} to 32.0 μg m^{-3}, and $\delta^{13}C_{-WSOC}$ varies between -26.24 ‰ to -23.35 ‰. ^{13}C is more enriched in WSOC than TC in the majority of the sampling period, indicating aged aerosols and/or ^{13}C depleted primary sources of non-WSOC component. Three haze events (e.g., namely the Episode 1, the Episode 2, the Episode 3) are identified with different tendencies of $\delta^{13}C_{-WSOC}$ during the accumulation of WSOC aerosols. Similar patterns of the WSOC concentrations and the $\delta^{13}C_{-WSOC}$ values in the Episode 1 are demonstrated to be affected by the air mass transported from northern China. The increase of $\delta^{13}C_{-WSOC}$ indicates that the WSOC aerosols from the studied site is subject to a substantial photochemical aging process during the long range transport. The contrasting trend of the WSOC and $\delta^{13}C_{-WSOC}$ values in the Episode 2 is interpreted as the contribution of regional C3

plants biomass burning sources. In the Episode 3, the heavier isotope (^{13}C) is clearly enriched in total carbon (TC) compares to WSOC fraction due to the dust contribution.

The optimized method is demonstrated to be accurate and precise to detect the WSOC mass concentration and its isotope compositions ($\delta^{13}C_{\text{-WSOC}}$) in aerosols. Our results indicate that the high time-resolved measurement of $\delta^{13}C_{\text{-WSOC}}$ can be used to distinguish different atmospheric processes such as photochemical aging and aerosol sources (e.g., biomass burning and dust). However, a quantitative understanding of sources and formation processes of WSOC aerosols is still of great challenge. To reduce the knowledge gaps, a combination of multiple methodologies is needed in future studies, such as high time-resolved measurement of radiocarbon (^{14}C) and stable carbon isotope compositions ($\delta^{13}C$), and the real-time measurement of chemical compositions (e.g., Aerosol Mass Spectrometers, AMS or Thermal Desorption Aerosol Gas Chromatograh-AMS).

Author contributions. YZ conceived and designed the study; YZ, FC and WZ designed the experimental strategy; WZ and YX performed the sampling and isotope measurements; YZ and WZ analyzed the experimental data; YZ and WZ proposed the hypotheses; WZ wrote manuscript with YL; all other co-authors contributed to writing.

Competing interests. The authors declare that they have no competing interests.

Acknowledgements. This study is supported by the National Key Research and Development Program of China (2017YFC0212704, 2017YFC0210101), the National Natural Science Foundation of China (Grant nos. 91644103, 41761144056, 41603104), Provincial Natural Science Foundation of Jiangsu (BK20170946), Foundation for Young Scientists of Jiangsu Province (BK20150895) and the funding of Jiangsu Innovation and Entrepreneurship Team.

Reference:

Agarwal, S., Aggarwal, S. G., Okuzawa, K., and Kawamura, K.: Size distributions of dicarboxylic acids, ketoacids, α-dicarbonyls, sugars, WSOC, OC, EC and inorganic ions in atmospheric particles over Northern Japan: Implication for long-range transport of Siberian biomass burning and East Asian polluted aerosols. Atmospheric Chemistry and Physics, 10(13), 5839–5858. https://doi.org/10.5194/acp-10-5839-2010,2010.

Aggarwal, S. G., and Kawamura, K.: Molecular distributions and stable carbon isotopic compositions of dicarboxylic acids and related compounds in aerosols from Sapporo, Japan: Implications for photochemical aging during long-range atmospheric transport. Journal of Geophysical Research Atmospheres, 113(14), 1–13. https://doi.org/10.1029/2007JD009365, 2008.

Anderson, C., Dibb, J. E., Griffin, R. J., and Bergin, M. H.: Simultaneous measurements of particulate and gas-phase water-soluble organic carbon concentrations at remote and urban-influenced locations. Geophysical Research Letters, 35(13), 2–5. https://doi.org/10.1029/2008GL033966, 2008.

Atkinson, R.: Kinetics and Mechanisms of the Gas-Phase Reactions of the Hydroxyl Radical with Organic Compounds under Atmospheric Conditions. Chemical Reviews 86(1), 69–201. https://doi.org/10.1021/cr00071a004,1986.

Bao, M., Cao, F., Chang, Y., Zhang, Y. L., Gao, Y., Liu, X., Zhang Y. Y., Zhang W. Q., Tang T. R., Xu Z. F., Liu S. D., Lee X. H., Li J., Zhang G.: Characteristics and origins of air pollutants and carbonaceous aerosols during wintertime haze episodes at a rural site in the yangtze river delta, china. Atmospheric Pollution Research, 8(5), 900-911, https://10.1016/j.apr.2017.03.001, 2017

Bauer, J. E., Haddad, R. I., Des Marais, D. J.: Method for determining stable isotope ratios of dissolved organic carbon in interstitial and other natural marine waters. Marine chemistry, 33(4): 335-351, https://doi.org/10.1016/0304-4203(91)90076-9, 1991.

Bozzetti, C., El Haddad, I., Salameh, D., Daellenbach, K. R., Fermo, P., Gonzalez, R., Minguillón, M. C., Iinuma, Y., Poulain, L., Elser, M., Müller, E., Slowik, J. G., Jaffrezo, J. L., Baltensperger, U., Marchand, N., and Prévôt, A. S. H.: Organic aerosol source apportionment by offline-AMS over a full year in Marseille, Atmos. Chem. Phys., 17, 8247-8268, 2017a.

Bozzetti, C., Sosedova, Y., Xiao, M., Daellenbach, K. R., Ulevicius, V., Dudoitis, V., Mordas, G., Byčenkienė, S., Plauškaitė, K., Vlachou, A., Golly, B., Chazeau, B., Besombes, J. L., Baltensperger, U., Jaffrezo, J. L., Slowik, J. G., El Haddad, I., and Prévôt, A. S. H.: Argon offline-AMS source apportionment of organic aerosol over yearly cycles for an urban, rural, and marine site in northern Europe, Atmos. Chem. Phys., 17, 117-141, 2017b.

Cai, Z., Jiang, F., Chen, J., Jiang, Z., and Wang, X.: Weather Condition Dominates Regional $PM_{2.5}$ Pollutions in the Eastern Coastal Provinces of China during Winter, Egu General Assembly Conference.969–980. https://doi.org/10.4209/aaqr.2017.04.0140, 2018.

Cao, J.J., Chow, J.C., Tao, J., Lee, S.C., Watson, J.G., Ho, K.F., Wang, G.H., Zhu, C.S. and Han, Y.M.: Stable carbon isotopes in aerosols from Chinese cities: Influence of fossil fuels. Atmospheric Environment, 45(6), 1359–1363. https://doi.org/10.1016/j.atmosenv.2010.10.056, 2011.

Chen, X.P., Zhou J.C., Wang X. R., Blackmer A. M., & Zhang F.: Optimal rates of nitrogen fertilization for a winter wheat-corn cropping system in northern china. Commun Soil Sci Plan, 35(3-4), 583-597, http:// 10.1081/CSS-120029734, 2004.

Currie, L. A., Klouda, G. A., Benner, B. A., Garrity, K., Eglinton, T. I.: Isotopic and molecular fractionation in combustion; three routes to molecular marker validation, including direct molecular 'dating' (GC/AMS). Atmospheric Environment, 33(17):2789-2806,http://doi: 10.1016/S1352-2310(98)00325-2, 1999.

Das, O., Wang, Y., Hsieh, Y. P.: Chemical and carbon isotopic characteristics of ash and smoke derived from burning of C and C grasses. Organic Geochemistry, 41(3):263-269, http://doi:10.1016/j.orggeochem.2009.11.001, 2010.

De Groot, P. A.: Handbook of stable isotope analytical techniques (Vol. 1). Elsevier, 2004.Decesari, S., Mircea, M., Cavalli, F., Fuzzi, S., Moretti, F., Tagliavini, E., and Facchini, M. C.:. Source attribution of water-soluble organic aerosol by nuclear magnetic resonance spectroscopy. Environmental Science and Technology, 41(7), 2479–2484. https://doi.org/Doi 10.1021/Es0617111, 2007.

Fisseha, R., Saurer, M., Jäggi, M., Siegwolf, R.T., Dommen, J., Szidat, S., Samburova, V. and Baltensperger, U.: Determination of primary and secondary sources of organic acids and carbonaceous aerosols using stable carbon isotopes. Atmospheric Environment, 43(2), 431–437. https://doi.org/10.1016/j.atmosenv.2008.08.041, 2009.

Fisseha R, Saurer M, Jäggi M, et al. Determination of stable carbon isotopes of organic acids and carbonaceous aerosols in the atmosphere.[J]. Rapid Communications in Mass Spectrometry Rcm, 2006, 20(15):2343-2347.

Fowler, K., Connolly, P. J., Topping, D. O., and O'Meara, S.: Maxwell–Stefan diffusion: a framework for predicting condensed phase diffusion and phase separation in atmospheric aerosol. Atmospheric Chemistry and Physics, 18(3), 1629–1642, 2018.

Gouw, J. A. D., Brock, C. A., Atlas, E. L., Bates, T. S., Fehsenfeld, F. C., & Goldan, P. D., Holloway J. S., Kuster W. C., Lerner B. M., Matthew B. M., Middlebrook A. M., Onasch T. B., Peltier R. E., Quinn P. K., Senff C. J., Stohl A., Sullivan A. P., Trainer M., Warneke C., Weber R. J., and Williams E. J.: Sources of particulate matter in the northeastern united states in summer: 1. direct emissions and secondary formation of organic matter in urban plumes. Journal of Geophysical Research Atmospheres, 113(D8), D08301. https:// doi:10.1029/2007JD009243, 2008.Hecobian, A., Zhang, X., Zheng, M., Frank, N., Edgerton, E. S., and Weber, R. J.: Water-soluble organic aerosol material and the light-absorption characteristics of aqueous extracts measured over the Southeastern United States. Atmospheric Chemistry and Physics, 10(13), 5965–5977. https://doi.org/10.5194/acp-10-5965-2010, 2010.

Huang, H., Ho, K.F., Lee, S.C., Tsang, P.K., Ho, S.S.H., Zou, C.W., Zou, S.C., Cao, J.J. and Xu, H.M.: Characteristics of carbonaceous aerosol in $PM_{2.5}$: Pearl Delta River region, China. Atmospheric research, 104, 227-236. https://doi.org/10.1016/j.atmosres.2011.10.016, 2012.

Huang, K., Zhuang, G., Li, J., Wang, Q., Sun, Y., Lin, Y., and Fu, J. S.: Mixing of Asian dust with pollution aerosol and the transformation of aerosol components during the dust storm over China in spring 2007. Journal of Geophysical Research, 115, D00K13. https://doi.org/10.1029/2009JD013145, 2010.

Huang, L., Brook, J.R., Zhang, W., Li, S.M., Graham, L., Ernst, D., Chivulescu, A. and Lu, G.: Stable isotope measurements of carbon fractions (OC/EC) in airborne particulate: A new dimension for source characterization and apportionment. Atmospheric Environment, 40(15), 2690–2705. https://doi.org/10.1016/j.atmosenv.2005.11.062, 2006.

Irei, S., Takami, A.,Hayashi, M., Sadanaga, Y., Hara, K., Kaneyasu, N., Sato K., Arakaki T., Hatakeyama S., Bandow H., Hikida T., and Shimono A.:Transboundary secondary organic aerosol in western japan indicated by the $\delta^{13}C$ of water-soluble organic carbon and the m/z 44

signal in organic aerosol mass spectra. Environmental Science & Technology, 48(11), 6273-6281, https://doi.org/10.1021/es405362y, 2014.

Jankowski, N., Schmidl, C., Marr, I. L., Bauer, H., and Puxbaum, H.: Comparison of methods for the quantification of carbonate carbon in atmospheric PM10 aerosol samples. Atmospheric Environment, 42(34), 8055–8064. https://doi.org/10.1016/j.atmosenv.2008.06.012, 2008.

Jimenez, J.L., Canagaratna, M.R., Donahue, N.M., Prevot, A.S.H., Zhang, Q., Kroll, J.H., DeCarlo, P.F., Allan, J.D., Coe, H., Ng, N.L. and Aiken, A.C.: Evolution of Organic Aerosols in the Atmosphere. Science, 326(5959), 1525–1529. https://doi.org/10.1126/science.1180353, 2009.

Kawamura, K., Kobayashi, M., Tsubonuma, N., Mochida, M., Watanabe, T., and Lee, M.: Organic and inorganic compositions of marine aerosols from East Asia: Seasonal variations of water-soluble dicarboxylic acids, major ions, total carbon and nitrogen, and stable C and N isotopic composition. Geochemical Society Special Publications, 9(C), 243–265. https://doi.org/10.1016/S1873-9881(04)80019-1, 2004.

Kirillova, E.N., Andersson, A., Sheesley, R.J., Kruså, M., Praveen, P.S., Budhavant, K., Safai, P.D., Rao, P.S.P. and Gustafsson, Ö.: ^{13}C- And ^{14}C-based study of sources and atmospheric processing of water-soluble organic carbon (WSOC) in South Asian aerosols. Journal of Geophysical Research Atmospheres, 118(2), 614–626. https://doi.org/10.1002/jgrd.50130, 2013.

Kirillova, E. N., Andersson, A., Tiwari, S., Kumar Srivastava, A., Singh Bisht, D., and Gustafsson, Ö.: Water-soluble organic carbon aerosols during a full New Delhi winter: Isotope-base source apportionment and optical properties. Journal of Geophysical Research D: Atmospheres, 119, 3476–3485. https://doi.org/10.1002/2013JD021272.Received, 2014.

Kirillova, E. N., Sheesley, R. J., Andersson, A., and Gustafsson, Ö. : Natural Abundance ^{13}C and ^{14}C Analysis of Water-Soluble Organic Carbon in Atmospheric. Analytical Chemistry, 82(19), 7973–7978. https://doi.org/10.1029/2006GL028325, 2010.

Kong, S., Li, X., Li, L., Yin, Y., Chen, K., Yuan, L., Zhang, Y., Shan, Y. and Ji, Y.: Variation of polycyclic aromatic hydrocarbons in atmospheric $PM_{2.5}$ during winter haze period around 2014 Chinese Spring Festival at Nanjing: Insights of source changes, air mass direction and firework particle injection. Science of the Total Environment, 520, 59–72. https://doi.org/10.1016/j.scitotenv.2015.03.001, 2015.

Lang, S. Q., Bernasconi, S. M., and Früh-Green, G. L.: Stable isotope analysis of organic carbon in small (μg C) samples and dissolved organic matter using a GasBench preparation device. Rapid Communications in Mass Spectrometry, 26(1), 9–16. https://doi.org/10.1002/rcm.5287, 2012.

Liang, L.L., Guenter, E., Duan, F.K., Ma, Y.L., Cheng, Y., Du, Z.Y. and He, K.B.: Composition and Source Apportionments of Saccharides in Atmospheric Particulate Matter in Beijing. Huanjing Kexue/Environmental Science 36, no. 11: 3935–42. https://doi.org/10.13227/j.hjkx.2015.11.001, 2015.

Martinelli, L. A., Camargo, P. B., Lara, L. B. L. S., Victoria, R. L., and Artaxo, P.: Stable carbon and nitrogen isotopic composition of bulk aerosol particles in a C4 plant landscape of southeast Brazil. Atmospheric Environment, 36(14), 2427–2432. https://doi.org/10.1016/S1352-2310(01)00454-X, 2002.

Martinez, R. E., Williams, B. J., Zhang, Y., Hagan, D., Walker, M., Kreisberg, N. M., Hering S. V., Hohaus T., Jayne J. T., Worsnop D. R.:. Development of a volatility and polarity separator

(VAPS) for volatility- and polarity-resolved organic aerosol measurement. Aerosol Science and Technology, 50(3), 255–271. https://doi.org/10.1080/02786826.2016.1147645, 2016.

Mills, N.L., Donaldson, K., Hadoke, P.W., Boon, N.A., MacNee, W., Cassee, F.R., Sandström, T., Blomberg, A. and Newby, D.E.: Adverse cardiovascular effects of air pollution. Nature Clinical Practice Cardiovascular Medicine, 6(1), 36–44. https://doi.org/10.1038/ncpcardio1399, 2009.

Miyazaki, Y., Fu, P, Q., Kawamura, K., Mizoguchi, Y., Yamanoi, K.: Seasonal variations of stable carbon isotopic composition and biogenic tracer compounds of water-soluble organic aerosols in a deciduous forest. Atmospheric Chemistry and Physics, 12:1367-1376, 10.1016/S0378-4274(98)80829-1, 2012.

Miyazaki, Y., Kawamura, K., Jung, J., Furutani, H., and Uematsu, M.: Latitudinal distributions of organic nitrogen and organic carbon in marine aerosols over the western North Pacific. Atmospheric Chemistry and Physics, 11(7), 3037–3049. https://doi.org/10.5194/acp-11-3037-2011, 2011.

Myhre, G.: Consistency between satellite-derived and modeled estimates of the direct aerosol effect. Science, 325(5937), 187–190. DOI: 10.1126/science.1174461, 2009.

Nina BrönicheOlsen, Ulstrup J . Quantum theory of kinetic isotope effects in proton transfer reactions[J]. Journal of the Chemical Society Faraday Transactions Physical Chemistry in Condensed Phases, 1979, 75(75):205-226.

Osada, K., Kido, M., Nishita, C., Matsunaga, K., Iwasaka, Y., & Nagatani, M., Nakada H.: Temporal variation of water-soluble ions of free tropospheric aerosol particles over central japan. Tellus Series B-chemical & Physical Meteorology, 59(4), 742–754, https://10.1111/j.1600-0889.2007.00296.x, 2007.

Park, S. S., Schauer, J. J., and Cho, S. Y.: Sources and their contribution to two water-soluble organic carbon fractions at a roadway site. Atmospheric Environment, 77, 348–357. https://doi.org/10.1016/j.atmosenv.2013.05.032, 2013.

Pathak, R. K., Wang, T., Ho, K. F., and Lee, S. C.: Characteristics of summertime PM2.5 organic and elemental carbon in four major Chinese cities: Implications of high acidity for water-soluble organic carbon (WSOC). Atmospheric Environment, 45(2), 318–325. https://doi.org/10.1016/j.atmosenv.2010.10.021, 2011.

Pavuluri, C. M., and Kawamura, K.: Evidence for 13-carbon enrichment in oxalic acid via iron catalyzed photolysis in aqueous phase. Geophysical Research Letters, 39(3), 1–6. https://doi.org/10.1029/2011GL050398, 2012.

Pavuluri C. M., Kawamura K.: Seasonal changes in TC and WSOC and their ^{13}C isotope ratios in Northeast Asian aerosols: land surface–biosphere–atmosphere interactions. Acta Geochimica, 36:355-358, http://doi.org/10.1007/s11631-017-0157-3, 2017.

Pavuluri, C. M., Kawamura, K., Swaminathan, T., and Tachibana, E.: Stable carbon isotopic compositions of total carbon, dicarboxylic acids and glyoxylic acid in the tropical Indian aerosols: Implications for sources and photochemical processing of organic aerosols. Journal of Geophysical Research Atmospheres, 116(18), 1–10. https://doi.org/10.1029/2011JD015617, 2011.

Polissar, P. J., Fulton, J. M., Junium, C. K., Turich, C. C., and Freeman, K. H.: Measurement of 13 C and 15 N Isotopic Composition on Nanomolar Quantities of C and N. Analytical Chemistry, 81(2), 755–763. https://doi.org/10.3354/meps240085.water, 2009.

Qin, X., Zhang, Z. F., Li, Y. W., Shen, Y., & Zhao, S. H... Sources analysis of heavy metal aerosol particles in north suburb of nanjing. Environmental Science. 37(12): 4467-4474, http://10.13227/j.hjkx.201605237,2016.

Ramanathan, V., Crutzen, P. J., Kiehl, J. T., and Rosenfeld, D.: Aerosols, climate, and the hydrological cycle. Science, 294(5549), 2119–2124. DOI: 10.1126/science.1064034, 2001.

Rudolph, J.: Gas Chromatography-Isotope Ratio Mass Spectrometry. Volatile Organic Compounds in the Atmosphere, 388–466. Blackwell Publishing: Oxford, UK, 2007.

Rudolph, J., Czuba, E., Norman, A. L., Huang, L., and Ernst, D.: Stable carbon isotope composition of nonmethane hydrocarbons in emissions from transportation related sources and atmospheric observations in an urban atmosphere. Atmospheric Environment, 36(7), 1173–1181. https://doi.org/10.1016/S1352-2310(01)00537-4, 2002.

Rudolph, J., Anderson R. S., Czapiewski K. V., Czuba E., Ernst D., Gillespie T., Huang L., Rigby C., and Thompson A. E.: The stable carbon isotope ratio of biogenic emissions of isoprene and the potential use of stable isotope ratio measurements to study photochemical processing of isoprene in the atmosphere. Journal of Atmospheric Chemistry, 44(1), 39–55, http://10.1023/A:1022116304550, 2003.

Saarikoski, S., Timonen, H., Saarnio, K., Aurela, M., Järvi, L., Keronen, P., Kerminen, V.M. and Hillamo, R.: Sources of organic carbon in fine particulate matter in northern European urban air. Atmospheric Chemistry and Physics, 8(20), 6281–6295. https://doi.org/10.5194/acp-8-6281-2008, 2008.

Sakugawa, H., Kaplan, I.R.: Stable carbon isotope measurements of atmospheric organic acids in Los Angeles, California. Geophysical Research Letters, 22, 1509–1512, https://doi.org/10.1029/95GL01359,1995

Sannigrahi, P., Sullivan, A. P., Weber, R. J., and Ingall, E. D.: Characterization of water-soluble organic carbon in urban atmospheric aerosols using solid-state C-13 NMR spectroscopy, Environ. Sci. Technol., 40, 666-672, 2006

Sharp, J. H.: Total organic carbon in seawater - comparison of measurements using persulfate oxidation and high temperature combustion. Marine Chemistry, 1(3), 211–229. https://doi.org/10.1016/0304-4203(73)90005-4, 1973.

Smith, B. N., and Epstein, S.: Two Categories of 13C/12C Ratios for Higher Plants. Plant Physiology, 47(3), 380–384. https://doi.org/10.1104/pp.47.3.380, 1971.

Sousa Moura, J. mauro, Martens, C. S., Moreira, M. Z., Lima, R. L., Sampaio, I. C. G., Mendlovitz, H. P., and Menton, M. C.: Spatial and seasonal variations in the stable carbon isotopic composition of methane in stream sediments of eastern Amazonia. Tellus B: Chemical and Physical Meteorology, 60(1), 21–31. https://doi.org/10.1111/j.1600-0889.2007.00322.x, 2008.

Sullivan, A. P., Weber, R. J., Clements, A. L., Turner, J. R., Bae, M. S., and Schauer, J. J.: A method for on-line measurement of water-soluble organic carbon in ambient aerosol particles: Results from an urban site. Geophysical Research Letters, 31(13), 14–17. https://doi.org/10.1029/2004GL019681, 2004.

Suto, N., Kawashima H.: Online wet oxidation/isotope ratio mass spectrometry method for determination of stable carbon isotope ratios of water‐soluble organic carbon in particulate

matter. Rapid Communications in Mass Spectrometry, 32(19): 1668-1674, http://doi.org/10.1002/rcm.8240, 2018.

Ten Brink, H., Maenhaut, W., Hitzenberger, R., Gnauk, T., Spindler, G., Even, A., Chi, X., Bauer, H., Puxbaum, H., Putaud, J.P. and Tursic, J: INTERCOMP2000: The comparability of methods in use in Europe for measuring the carbon content of aerosol. Atmospheric Environment, 38(38), 6507–6519. https://doi.org/10.1016/j.atmosenv.2004.08.027, 2004.

Trolier, M. , White, J. W. C., Tans, P. P., Masarie, K. A., Gemery, P. A.: Monitoring the isotopic composition of atmospheric CO_2: Measurements from the NOAA Global Air Sampling Network. Journal of Geophysical Research: Atmospheres, 101(D20), https://doi.org/10.1029/96JD02363, 1996.

Turekian, V. C., Macko, S., Ballentine, D., Swap, R. J., Garstang, M.: Causes of bulk carbon and nitrogen isotopic fractionations in the products of vegetation burns: Laboratory studies. Chemical Geology, 152(1-2):181-192. http://doi.10.1016/S0009-2541(98)00105-3, 1998.

Wang, G., Xie, M., Hu, S., Gao, S., Tachibana, E., and Kawamura, K.: Dicarboxylic acids, metals and isotopic compositions of C and N in atmospheric aerosols from inland China: Implications for dust and coal burning emission and secondary aerosol formation. Atmospheric Chemistry and Physics, 10(13), 6087–6096. https://doi.org/10.5194/acp-10-6087-2010, 2010.

Wang, H., Kawamura, K., and Shooter, D.: Wintertime organic aerosols in Christchurch and Auckland, New Zealand: Contributions of residential wood and coal burning and petroleum utilization. Environmental Science and Technology, 40(17), 5257–5262. https://doi.org/10.1021/es052523i, 2006.

Wang, Y., Jia, C., Tao, J., Zhang, L., Liang, X., Ma J., Gao H., Huang T., Zhang K.:Chemical characterization and source apportionment of pm2.5 in a semi-arid and petrochemical-industrialized city, northwest china. Science of The Total Environment, 573, 1031-1040, 10.1016/j.scitotenv.2016.08.179,2016.

Weber, R. J., Sullivan, A. P., Peltier, R. E., Russell, A., Yan, B., Zheng, M., de Gouw, J., Warneke, C., Brock, C., Holloway, J. S., Atlas, E. L., and Edgerton, E.: A study of secondary organic aerosol formation in the anthropogenic-influenced southeastern United States, J. Geophys. Res., 112, D13302, 2007.

Werner, R. A., Bruch, B. A., and Brand, W. A.: ConFlo III - an interface for high precision $\delta^{13}C$ and $\delta^{15}N$ analysis with an extended dynamic range. Rapid Communications in Mass Spectrometry, 13(13), 1237–1241. https://doi.org/10.1002/(SICI)1097-0231(19990715)13:13<1237::AID-RCM633>3.0.CO;2-C, 1999.

Widory, D.: Combustibles, fuels and their combustion products: A view through carbon isotopes. Combustion Theory and Modelling, 10(5), 831–841. https://doi.org/10.1080/13647830600720264, 2006.

Wozniak, A. S., Bauer, J. E., Sleighter, R. L., Dickhut, R. M., and Hatcher, P. G.: Molecular characterization of aerosol-derived water soluble organic carbon using ultrahigh resolution electrospray ionization Fourier transform ion cyclotron resonance mass spectrometry. Atmospheric Chemistry and Physics, 8(2), 5099–5111. https://doi.org/10.5194/acp-8-5099-2008, 2008.

Yu, S., Zhang, Q., Yan, R., Wang, S., Li, P., & Chen, B.,Liu W., Zhang X.: Origin of air pollution during a weekly heavy haze episode in hangzhou, china. Environmental Chemistry Letters, 12(4), 543-550, 10.1007/s10311-014-0483-1, 2014.

Zeng, Y., & Hopke, P. K.: A study of the sources of acid precipitation in ontario, canada. Atmospheric Environment, 23(7), 1499-1509, 10.1016/0004-6981(89)90409-5,1989.

Zhang, F., Cheng, H. R., Wang, Z. W., Lv, X. P., Zhu, Z. M., & Zhang, G., et al.: Fine particles (pm 2.5) at a cawnet background site in central china: chemical compositions, seasonal variations and regional pollution events. Atmospheric Environment, 86(3), 193-202, 10.1016/j.atmosenv.2013.12.008, 2014.

Zhang, R., Jing, J., Tao, J., Hsu, S. C., Wang, G., & Cao, J. J., Lee C. S. L., Zhu L., Chen Z. M., Zhao Y., Shen Z. X.: Chemical characterization and source apportionment of pm2.5 in Beijing: seasonal perspective. Atmospheric Chemistry and Physics, 13(14), 7053-7074, 10.5194/acp-13-7053-2013, 2013.

Zhang, Y.L., El-Haddad, I., Huang, R.J., Ho, K.F., Cao, J.J., Han, Y.M., Zotter, P., Bozzetti, C., Daellenbach, K.R., Slowik, J.G., Salazar, G., Prévôt, A.S. and Szidat, S.: Large contribution of fossil fuel derived secondary organic carbon to water soluble organic aerosols in winter haze in China. Atmospheric chemistry and physics, 18(6), pp.4005-4017. https://doi.org/10.5194/acp-18-4005-2018, 2018.

Zhang, Y.L., Li, J., Zhang, G., Zotter, P., Huang, R.J., Tang, J.H., Wacker, L., Prévôt, A.S. and Szidat, S.: Radiocarbon-based source apportionment of carbonaceous aerosols at a regional background site on Hainan Island, South China. Environmental Science and Technology, 48(5), 2651–2659. https://doi.org/10.1021/es4050852, 2014.

Zhou, Y., Guo, H., Lu, H., Mao, R., Zheng, H., and Wang, J.: Analytical methods and application of stable isotopes in dissolved organic carbon and inorganic carbon in groundwater. Rapid Communications in Mass Spectrometry, 29(19), 1827–1835. https://doi.org/10.1002/rcm.7280, 2015.

Table 1. Various blank preparation with results.

Identifier	Oxidant [a]	Acid [b]	C content (μgC)	$\delta^{13}C$(‰)
Mili-Q water	-	-	ND*	-
Mili-Q water	-	-	ND*	-
Mili-Q water +Acid-1	-	100 uL 85 % H_3PO_4, AR	0.04	-1.6
Mili-Q water +Acid-1	-	100 uL 85 % H_3PO_4, AR	0.04	-4.3
Mili-Q water +Acid-2	-	100 uL 85 % H_3PO_4, HPLC	0.03	-4.9
Mili-Q water +OX+Acid-1	2.0 g $K_2S_2O_8$	100 uL 85 % H_3PO_4, AR	0. 63	-25.90
Mili-Q water +OX+Acid-1	2.0 g $K_2S_2O_8$	100 uL 85 % H_3PO_4, AR	0.54	-25.69
Mili-Q water +OX+Acid-1	2.0 g $K_2S_2O_8$	100 uL 85 % H_3PO_4, AR	0.46	-24.77
Mili-Q water +OX+Acid-2	2.0 g $K_2S_2O_8$	100 uL 85 % H_3PO_4, HPLC	0.63	-26.66
Mili-Q water +OX+Acid-2	2.0 g $K_2S_2O_8$	100 uL 85 % H_3PO_4, HPLC	0.56	-27.38
Mili-Q water +OX+Acid-2	2.0 g $K_2S_2O_8$	100 uL 85 % H_3PO_4, HPLC	0.58	-26.91

[a, b] oxidant and acid are added to 50 mL Mili-Q water.

ND* : Not detected

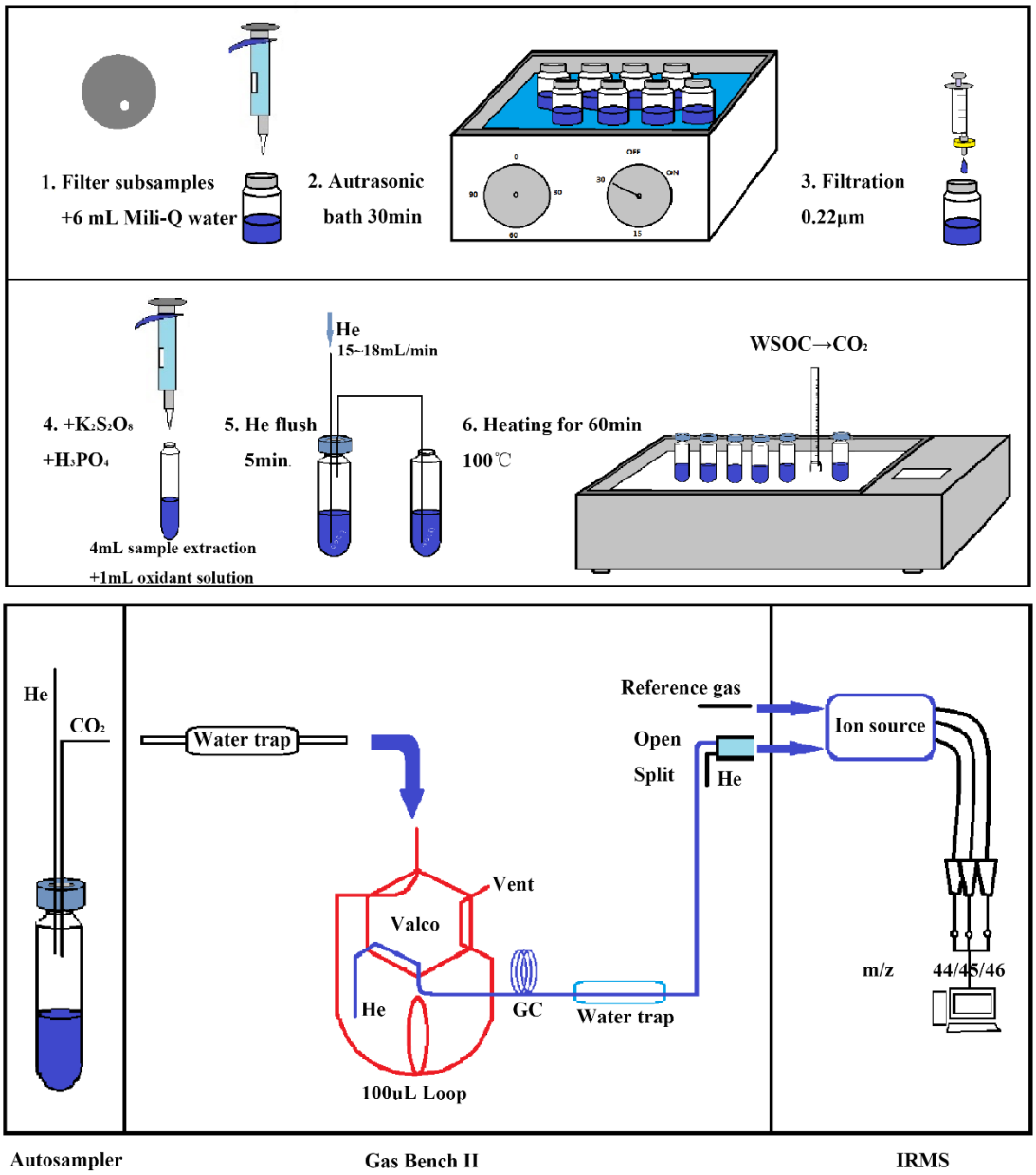

Figure 1. Schematic of the optimized method for the measurement of WSOC mass concentrations and the $\delta^{13}C_{-WSOC}$ values. (A filter disc is dissolved with 6mL Mili-Q water in a 20 mL pre-combusted glass bottle in the first step. After 30 minutes autrasonic bath, the WSOC extract is filtered with 0.22 μm syringe filter and transferred to another 20 mL pre-combusted glass bottle in step 3. 4 mL filtrate is transferred to a 12 mL pre-combusted glass vial which contains 1 mL oxidant solution (2.0g $K_2S_2O_8$ and 100 μL 85% H_3PO_4 dissolved in 50 mL Mili-Q water) in the vial in step 4. Next, the mixed solution of WSOC extract and the oxidant solution is flushed with Helium at a flow rate of 15-18 mL min^{-1} as shown in step 5. At last, the vials are heated for 60 minutes under 100 ℃ in the sand bath pot (step 6).)

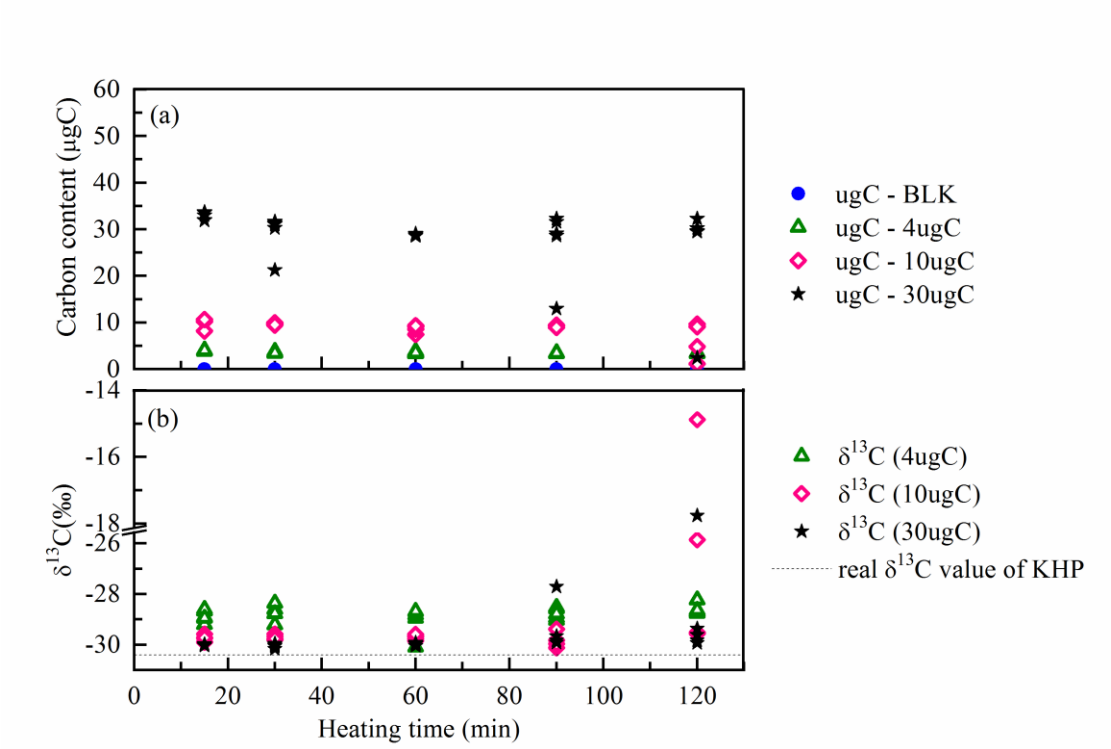

Figure 2. Carbon contents (a) and isotopic ratios (b) of KHP after different heating time.

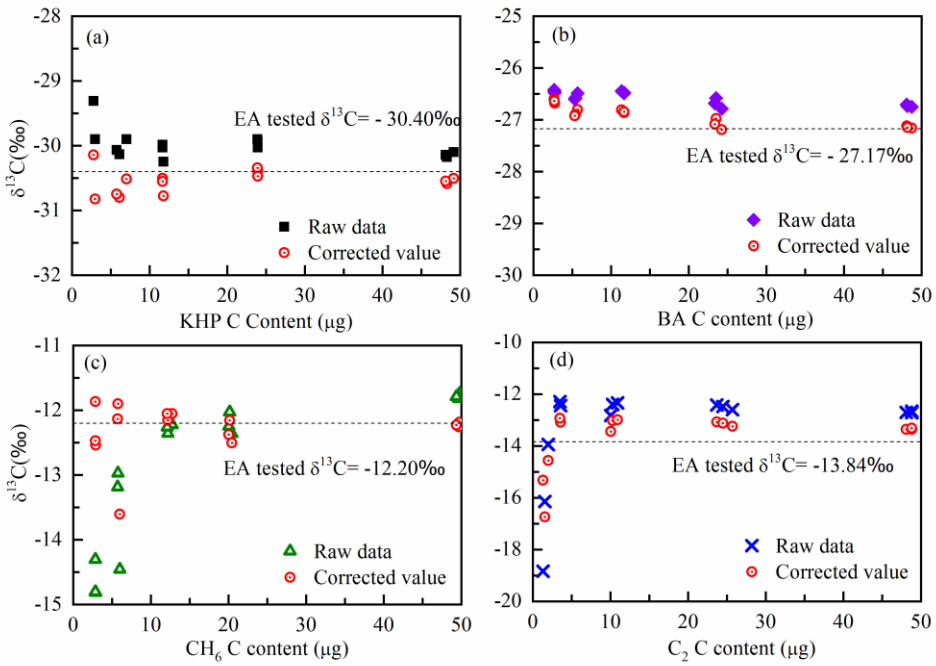

Figure 3. Isotope results before and after the two-step correction of the four standards. (a. KHP, b. BA, c. CH_6, d. C_2. Red circle with a spot represents the two-step corrected isotopic ratios; ■,◆,△,× represent the raw data from Gas Bench II; the dotted line represents the blank corrected $\delta^{13}C$ values tested by EA)

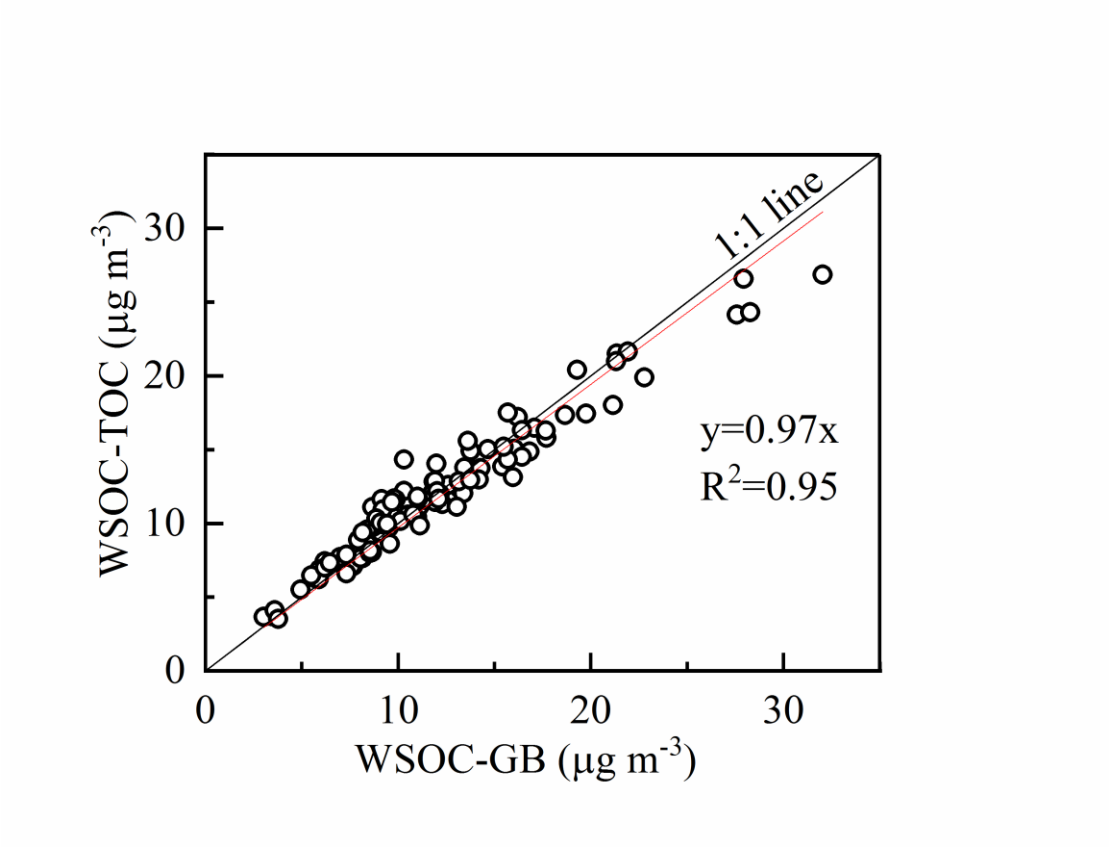

925

926 **Figure 4.** Correlation of WSOC mass concentrations measured with Gas Bench II - IRMS and

927 TOC analyzer.

928

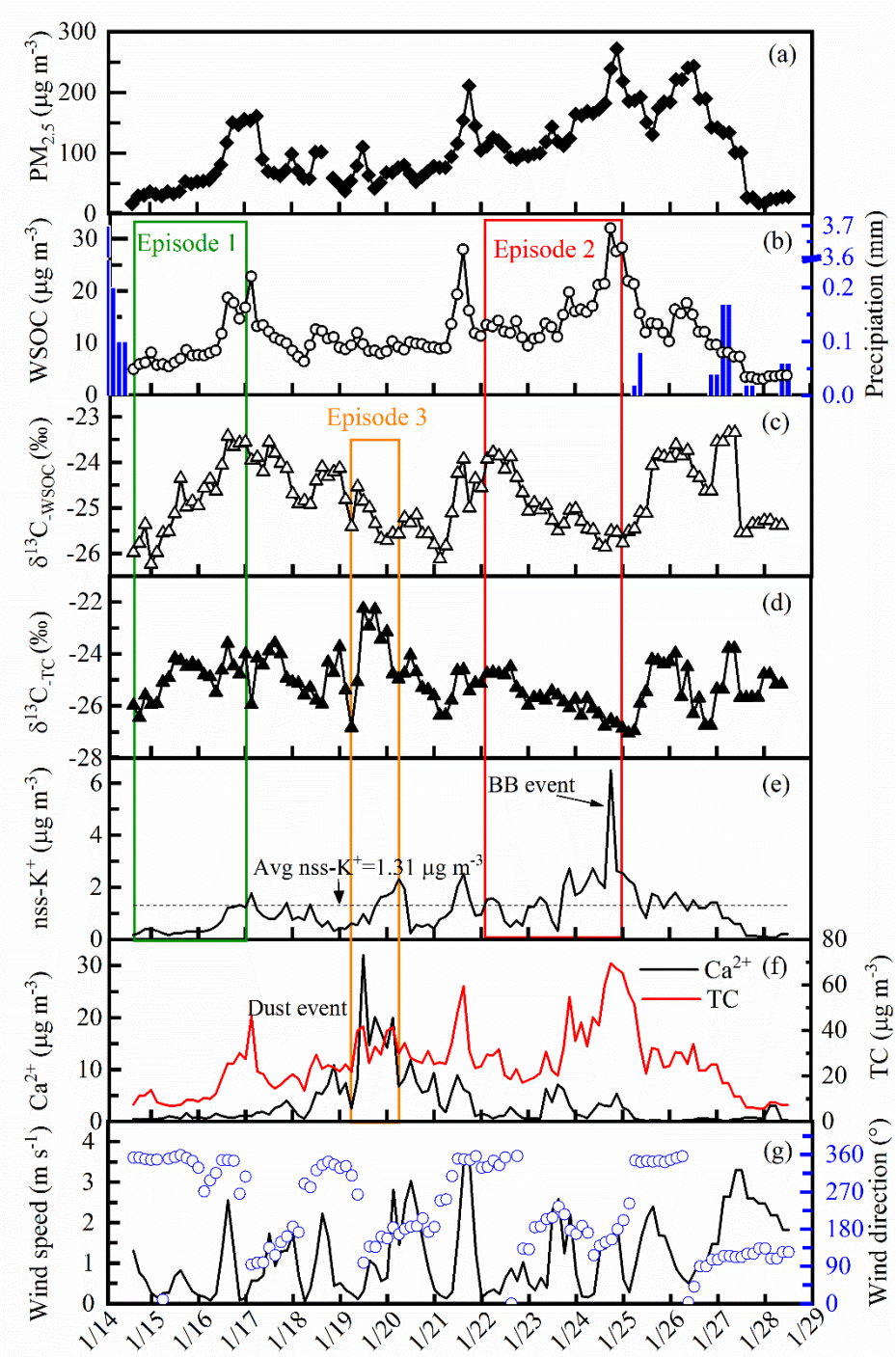

Figure 5. Time series of $PM_{2.5}$, WSOC, precipitation, $\delta^{13}C$ values, nss-K^+, Ca^{2+}, TC, wind speed and wind direction at the sampling site during the studied period. (The time period framed with the rectangles is defined as the Episode 1 (green), the Episode 2 (red) and the Episode 3 (orange). The dotted line in 5e is the average value of nss-K^+ during the studied period. The high concentration and intense increase of nss-K^+ in the Episode 2 indicate a significant biomass burning (BB) event, and is marked with "BB event" in 5e. The similar trends of Ca^{2+} and TC suggest a dust event in the Episode 3.**)**

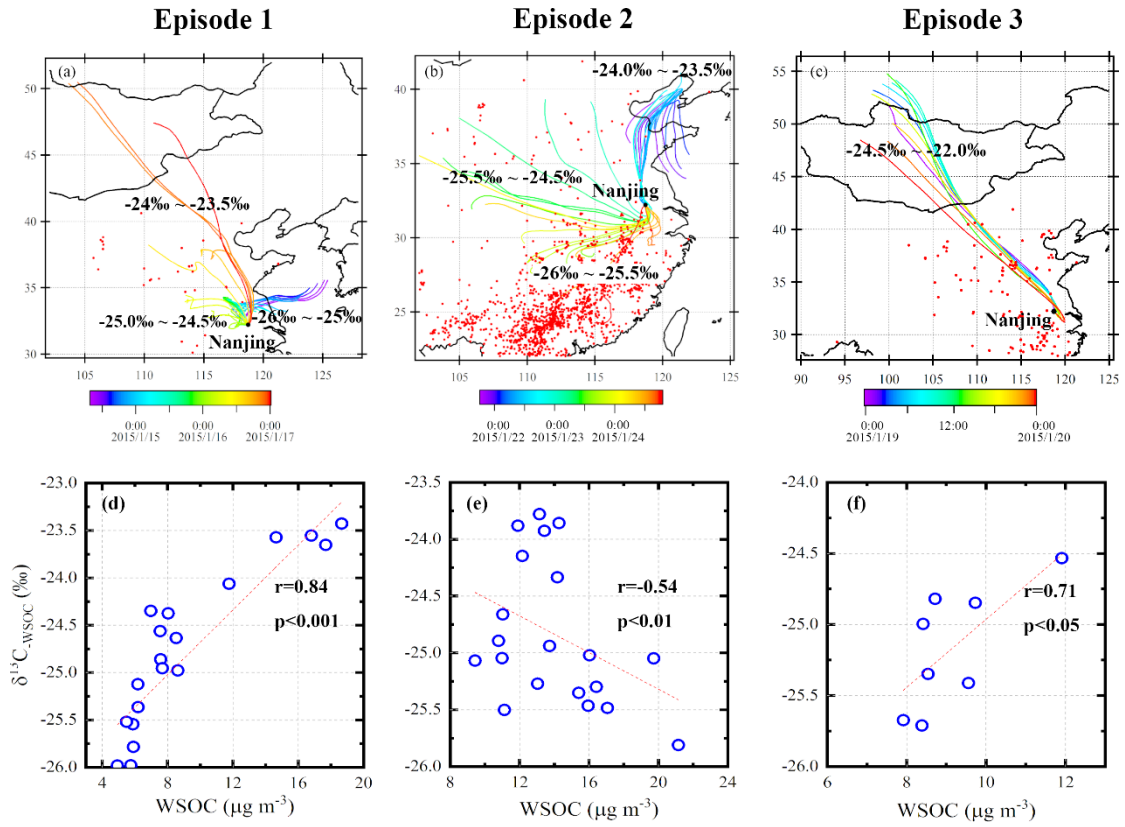

Figure 6. 48h-air mass back trajectories at 500m and MODIS fire maps in the three episodes and the corresponding relationship between WSOC and $\delta^{13}C_{\text{-WSOC}}$.

(a, b and c represent the back trajectories and the fire maps of the Episode 1, 2 and 3, separately. The colors of the back trajectories are marked according to the time of the specific trajectory. Red points represent the fire spots in each episode obtained from the Fire Information for Resource Management System (FIRMS) derived from the Moderate Resolution Imaging Spectroradiometer. The ranges of the $\delta^{13}C$ values of the back trajectories are labeled: the marked isotopic ratios are the $\delta^{13}C_{\text{-WSOC}}$ values (for a and b) and the $\delta^{13}C_{\text{-TC}}$ values (for c). d, e and f are the correlation between WSOC and $\delta^{13}C_{\text{-WSOC}}$ in each episode.)

Supporting information for the article entitled

High time-resolved measurement of stable carbon isotope composition in water-soluble organic aerosols: method optimization and a case study during winter haze in East China

Wenqi Zhang[1,2,3], Yan-Lin Zhang[1,2,3]*, Fang Cao[1,2,3], Yankun Xiang[1,2,3], Yuanyuan Zhang[1,2,3], Mengying Bao[1,2,3], Xiaoyan Liu[1,2,3], Yu-Chi Lin[1,2,3]

1Yale–NUIST Center on Atmospheric Environment, International Joint Laboratory on Climate and Environment Change (ILCEC), Nanjing University of Information Science and Technology, Nanjing 210044, China

2Key Laboratory of Meteorological Disaster, Ministry of Education (KLME)/ Collaborative Innovation Center on Forecast and Evaluation of Meteorological Disasters (CIC-FEMD), Nanjing University of Information Science and Technology, Nanjing 210044, China

3Jiangsu Provincial Key Laboratory of Agricultural Meteorology, College of Applied Meteorology, Nanjing University of Information Science and Technology, Nanjing 210044, China

7 Pages

1 Table

5 Figures

Table S1. Statistical results of isotope compositions after different heating time.

Heating time	Carbon content	Average $\delta^{13}C$	SD (n=5)	Total SD
15	0	-32.01		0.53
	4	-28.86	0.24	
	10	-29.77	0.13	
	30	-30.00	0.02	
30	0	-32.50		0.57
	4	-28.92	0.53	
	10	-29.71	0.09	
	30	-30.04	0.08	
60	0	-31.03		0.51
	4	-29.04	0.59	
	10	-29.71	0.10	
	30	-29.96	0.05	
90	0	-32.47		0.71
	4	-28.77	0.22	
	10	-29.85	0.28	
	30	-29.39	0.94	
120	0	-29.13		4.58
	4	-28.59	0.21	
	4	-26.42	6.46	
	30	-27.30	5.34	

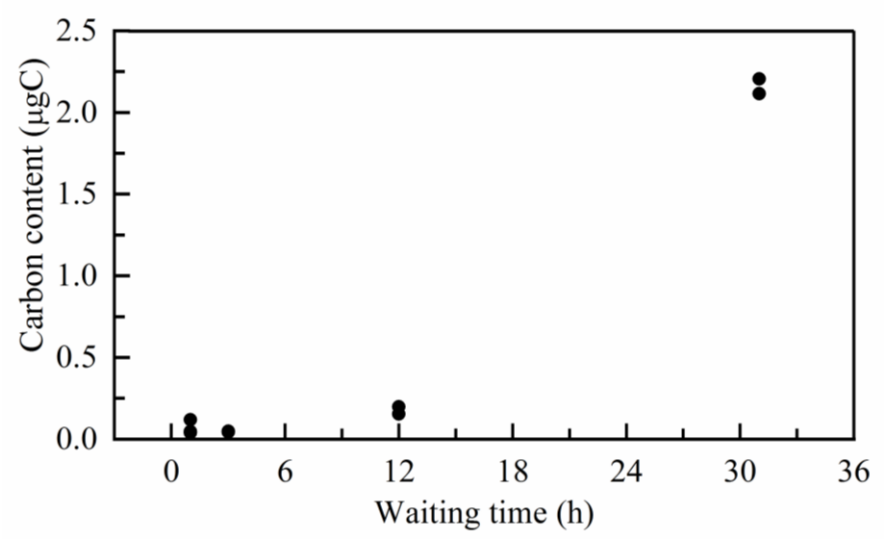

Figure S1. Carbon contents of one ambient aerosol sample replicates tested after different waiting time (duration between the mixture of aerosol extractions with the oxidizing solution and the helium flushing step) without heating.

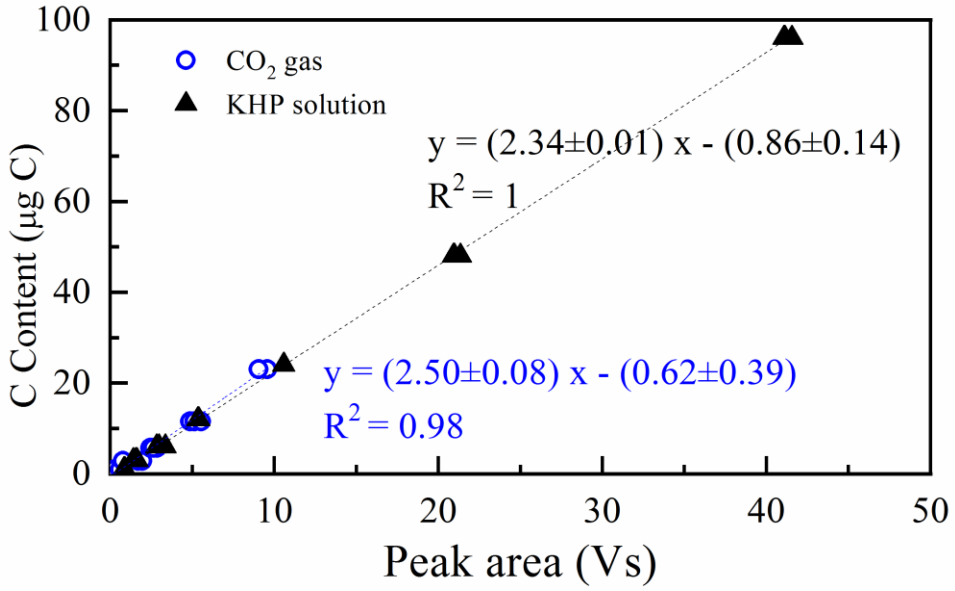

Figure S2. Standard curve to quantify the unknown samples.

(The standard curve is established by the CO_2 gas / the KHP solution and the input carbon content of the certain vials. The blue dotted line is the linear fit of the results of CO_2 gas, and the black dotted line is the linear fit of the results of KHP solution.)

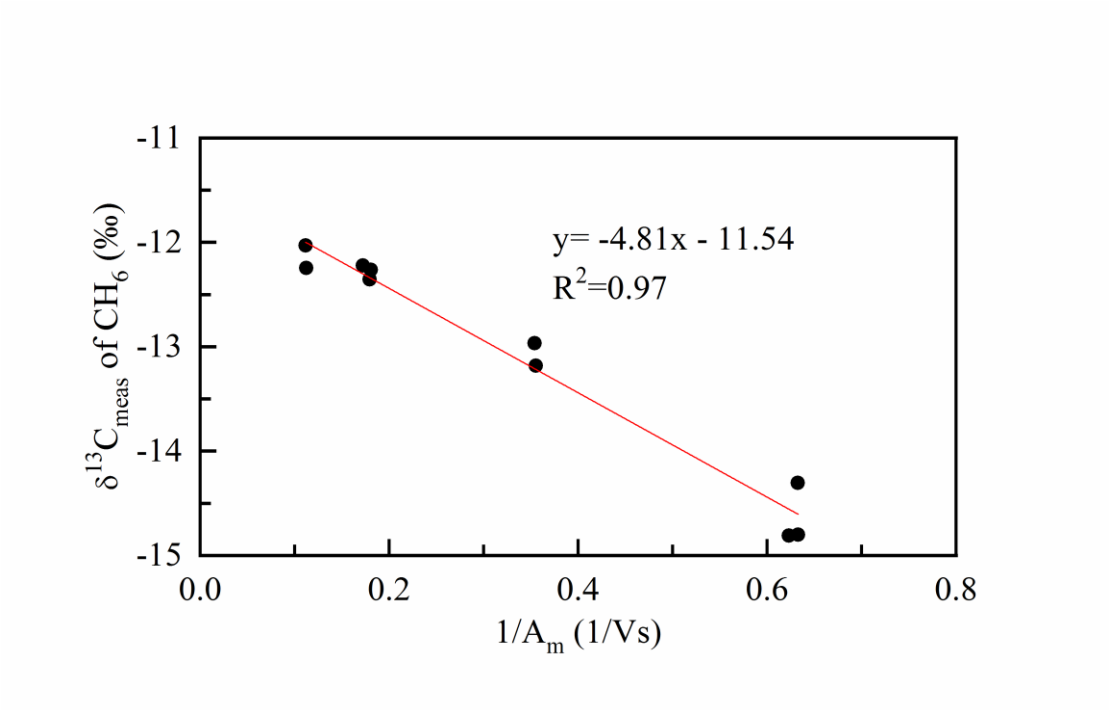

Figure S3. Relationship between the values of $1/A_m$ and $\delta^{13}C$ obtained from the measurement of CH_6.

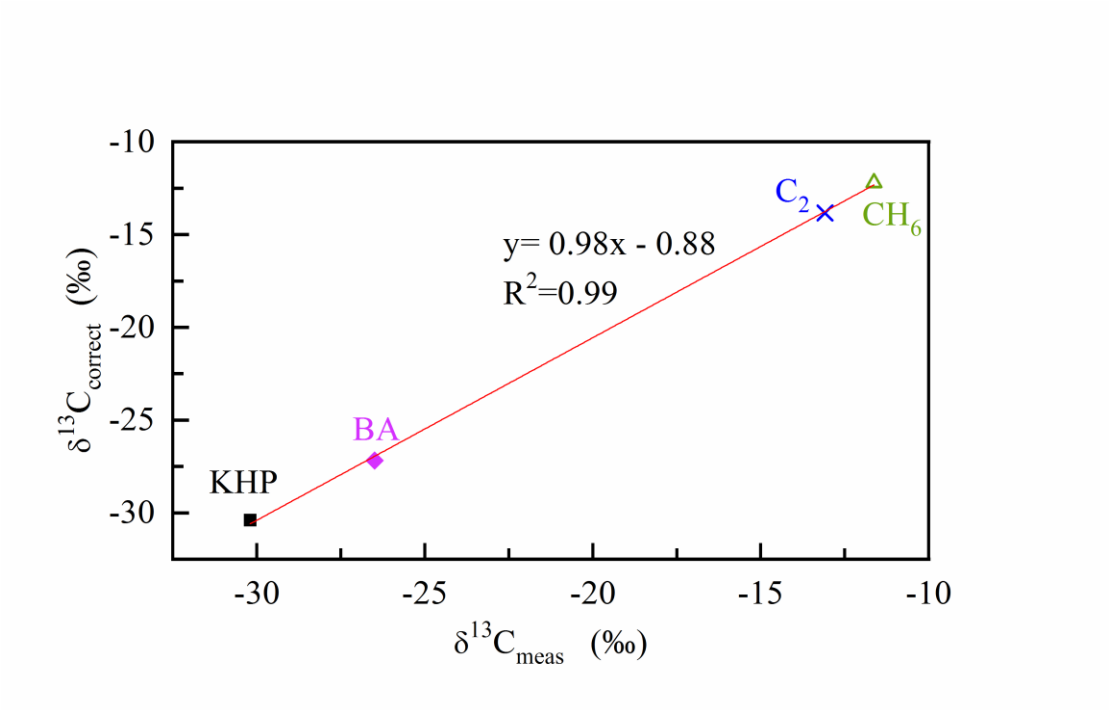

Figure S4. Calibration curve of the isotope composition for the correction of the systematic bias. (The values of y axis are the correct isotope values of the standards measured with EA using combustion method without pretreatment, and the values of x axis are the measured isotope results of the standards obtained from the wet oxidation method and determined with Gas Bench II.)

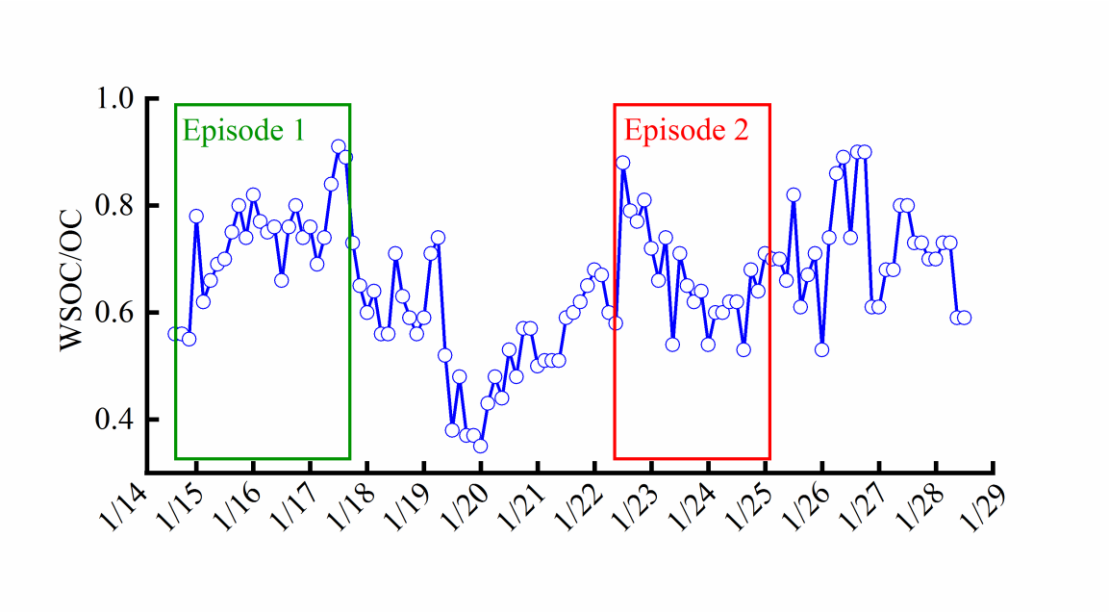

Figure S5. Time series of WSOC/OC.